Scattering problem in the Nanofiber Trapped Atom system

Xiaodong Qi and Ben Quinn Baragiola

January 29, 2014

Abstract

This is a study on the Nanofiber Trapped Atoms project (NaTA) in the perspective of scattering.

Chapter 1

One atom trapped aside a nanofiber

1.1 Green function for the classical light

In this section, we look at the case that only one atom is trapped aside the nanofiber. To be specific, we consider the following scenario: a laser beam propagates through a nanofiber along z direction; a Cesium (Cs) atom (can be other atoms) allocates at $\mathbf{r}_{atom} = \mathbf{r}'$ close by the nanofiber, and responds to the optical field. Due to the response of the atom, a light is re-emitted from the atom with a phase shift propagating in all directions, and interferes with the guided mode, which causes attenuation and a change of the index of refraction of the nanofiber effectively.

We assume that the nanofiber is a infinite long cylinder with a radium of a (in our cases, $a < \lambda$, where λ is the wavelength of the laser beam). The laser beam propagating in the nanofiber generates an electrical field given by

$$\mathbf{E}_0(\mathbf{r}, t) = \boldsymbol{\mathcal{E}}_0(\mathbf{r})e^{-i\omega t} = \mathcal{E}_0(\mathbf{r})\mathbf{u}_0(\mathbf{r})e^{-i\omega t}, \tag{1.1}$$

where ω is the angular frequency and $\boldsymbol{\mathcal{E}}_0(\mathbf{r}) = \mathcal{E}_0\mathbf{u}_0$ is the positive-frequency electric field envelope, with $\mathcal{E}_0(\mathbf{r})$ and $\mathbf{u}_0(\mathbf{r})$ being the field amplitude and the polarization vector at $\mathbf{r}$, respectively. In general, $\mathcal{E}(\mathbf{r})$ is a complex scalar and $\mathbf{u}(\mathbf{r})$ is a complex unit vector.

We assume the nanofiber is a linear medium with no absorption to the traveling wave. The refractive intrinsic index of the nanofiber can be given by

$$n_0(\mathbf{r}) = \begin{cases} n_1 = 1.46, & r_\perp \le a, \\ n_2 = 1, & r_\perp > a, \end{cases} \tag{1.2}$$

where we have set the z-axis to be the symmetric center of the nanofiber and $r_\perp = \sqrt{x^2 + y^2}$. We would like to determine the form of the scattered field

$\boldsymbol{\mathcal{E}}_s(\mathbf{r})$, and the total field $\boldsymbol{\mathcal{E}}(\mathbf{r}) = \boldsymbol{\mathcal{E}}_0(\mathbf{r}) + \boldsymbol{\mathcal{E}}_s(\mathbf{r})$. Formally, the total time-dependent electrical field can be rewritten as

$$\mathbf{E}(\mathbf{r}, t) = \boldsymbol{\mathcal{E}}(\mathbf{r})e^{-i\omega t} = \mathcal{E}(\mathbf{r})\mathbf{u}(\mathbf{r})e^{-i\omega t}, \tag{1.3}$$

The total field will satisfy the *Maxwell-Helmholtz equation* that

$$\left[\nabla \times \nabla \times -\frac{\omega^2}{c^2}n^2(\mathbf{r})\right]\boldsymbol{\mathcal{E}}(\mathbf{r}) = 0. \tag{1.4}$$

Notice that the total index of refraction $n(\mathbf{r})$ we used above has already included the scattering effect caused by the atom on the nanofiber, which usually has a complicated form. It is not in general possible to solve the differential equation as given above. The solution to the Maxwell-Helmholtz equation with $n(\mathbf{r}) = 1$, however, are much more tractable, so we subtract $\frac{\omega^2}{c^2}\boldsymbol{\mathcal{E}}(\mathbf{r})$ to each side of Equ. 1.4 and add $\frac{\omega^2}{c^2}n(\mathbf{r})\boldsymbol{\mathcal{E}}(\mathbf{r})$ to give

$$\left[\nabla \times \nabla \times -\frac{\omega^2}{c^2}\right]\boldsymbol{\mathcal{E}}(\mathbf{r}) = \frac{\omega^2}{c^2}\boldsymbol{\chi}(\mathbf{r})\boldsymbol{\mathcal{E}}(\mathbf{r}), \tag{1.5}$$

where we have defined the electric susceptibility $\boldsymbol{\chi}(\mathbf{r}) = n^2(\mathbf{r}) - 1 = \varepsilon_r(\mathbf{r}) - 1 = \delta(\mathbf{r} - \mathbf{r}')\boldsymbol{\alpha}\,(r_\perp > a)$ where $\varepsilon_r(\mathbf{r})$ is the relative permittivity or dielectric constant at $\mathbf{r}$ and $\boldsymbol{\alpha}$ is the polarizability of the atom [1]. This equation above has a source term

$$S(\mathbf{r}) = \frac{\omega^2}{c^2}\boldsymbol{\chi}(\mathbf{r}), \tag{1.6}$$

and can be solved by solving the corresponding Green function in the frequency domain

$$\left[\nabla \times \nabla \times -\frac{\omega^2}{c^2}\right]\mathbf{G}(\mathbf{r}, \mathbf{r}') = \mathbf{I}\delta(\mathbf{r} - \mathbf{r}'). \tag{1.7}$$

The solution for the Green function in free space is

$$\mathbf{G}(\mathbf{r}, \mathbf{r}') = \frac{e^{i\mathbf{k}\cdot(\mathbf{r}-\mathbf{r}')}}{|\mathbf{r} - \mathbf{r}'|}. \tag{1.8}$$

Assuming the boundary contributions vanish, we may have

$$\boldsymbol{\mathcal{E}}(\mathbf{r}) = \boldsymbol{\mathcal{E}}_0(\mathbf{r}) + \int_V S(\mathbf{r}')\boldsymbol{\mathcal{E}}(\mathbf{r}')\frac{e^{i\mathbf{k}\cdot\mathbf{R}}}{R}\mathrm{d}^3 r', \tag{1.9}$$

where $\boldsymbol{\mathcal{E}}_0(\mathbf{r})$ is the homogeneous Maxwell-Helmholtz equation in the limit that $S(\mathbf{r}) \longrightarrow 0$, $\mathbf{R} = \mathbf{r} - \mathbf{r}'$. Therefore, the scattering field is

$$\boldsymbol{\mathcal{E}}_s(\mathbf{r}) = \int_V S(\mathbf{r}')\boldsymbol{\mathcal{E}}(\mathbf{r}')\frac{e^{i\mathbf{k}\cdot\mathbf{R}}}{R}\mathrm{d}^3 r' \tag{1.10}$$

[1] This electric susceptibility needs to be fixed. Aside on multiple atoms case: if there are many atoms distributed along the nanofiber, we can in general use $\boldsymbol{\chi}(\mathbf{r}) = \sum_i \delta(\mathbf{r} - \mathbf{r}_i)\boldsymbol{\alpha}^i$, where i counts over all atoms.

$$= \int_V \frac{\omega^2}{c^2} \boldsymbol{\chi}(\mathbf{r}') \boldsymbol{\mathcal{E}}(\mathbf{r}') \frac{e^{i\mathbf{k}\cdot\mathbf{R}}}{R} \mathrm{d}^3 r'. \tag{1.11}$$

In general, scattering problems cannot be solved analytically, due to the presence of the complicated scattered field. By the use of Green function method, we have converted our differential equation for the scattered field into volume integral equations. They are very important since they form the basis for various formalisms such as the *method of moments*, the *Lippmann-Schwinger equation*, and the *coupled dipole method*. In general, these integral equations can be solved numerically using the methods mentioned above. Alternatively, we may develop a LiouvilleNeumann series solution to the equation, namely the Born series.

The Born series is typically derived by assuming that the scattering potential is very weak, and may be written as $S(\mathbf{r}) \to \delta S(\mathbf{r})$, where δ is a dimensionless parameter, which ultimately will be set to be 1 to obtain the solution of the electrical field. We then seek a series solution for the total field of the form

$$\boldsymbol{\mathcal{E}}(\mathbf{r}) = \sum_{n=0}^{\infty} \delta^n \mathbf{V}_n(\mathbf{r}). \tag{1.12}$$

On substituting the expression above into Equ. 1.9, we find the series

$$\mathbf{V}_0 = \boldsymbol{\mathcal{E}}_0, \tag{1.13}$$

$$\mathbf{V}_1 = \int_V S(\mathbf{r}') \boldsymbol{\mathcal{E}}_0 \frac{e^{i\mathbf{k}\cdot\mathbf{R}}}{R} \mathrm{d}^3 r', \tag{1.14}$$

$$\ldots\ldots \tag{1.15}$$

$$\mathbf{V}_n = \int_V S(\mathbf{r}') \boldsymbol{\mathcal{E}}_{n-1} \frac{e^{i\mathbf{k}\cdot\mathbf{R}}}{R} \mathrm{d}^3 r', \tag{1.16}$$

where the *Born approximation* only includes up to the first-order term. Under the Born approximation, the solution for the electrical field with one single atom can be given by

$$\boldsymbol{\mathcal{E}}(\mathbf{r}) = \boldsymbol{\mathcal{E}}_0(\mathbf{r}) + \int_V S(\mathbf{r}') \boldsymbol{\mathcal{E}}_0(\mathbf{r}') \frac{e^{i\mathbf{k}\cdot\mathbf{R}}}{R} \mathrm{d}^3 r' \tag{1.17}$$

$$= \boldsymbol{\mathcal{E}}_0(\mathbf{r}) + \frac{\omega^2}{c^2} \boldsymbol{\alpha}(\mathbf{r}') \boldsymbol{\mathcal{E}}_0(\mathbf{r}') \frac{e^{i\mathbf{k}\cdot(\mathbf{r}-\mathbf{r}')}}{|\mathbf{r}-\mathbf{r}'|}, \tag{1.18}$$

where $\boldsymbol{\alpha}(\mathbf{r}')$ denotes the polarizability of the atom at $\mathbf{r}'$.

Notice that Born series does not necessarily converge. Usually, we need to verify if the perturbation fields are much weaker than the field $\boldsymbol{\mathcal{E}}_0$ before using Born series.

To be continued: Retard Green function for forward and backward solutions, Green function with a proper boundary condition for the nanofiber...

1.2 Paraxial expansion of the mode

In the case that the light fields propagate along a certain direction z and spread out only slowly in the transverse direction, we can use the *paraxial approxima-*

tion to simplify the light propagation problem, especially the analytical integral of the Fourier integrals of the fields. In that case, the z component of the wavevectors can be expanded in a series as

$$k_z = k\sqrt{1-(k_x^2+k_y^2)/k^2} \approx k - \frac{(k_x^2+k_y^2)}{2k}. \tag{1.19}$$

This reflects the physical fact that the wavevectors $\mathrm{k} = (k_x, k_y, k_z)$ in the angular spectrum representation are almost parallel to the z-axis and the transverse wavenumbers (k_x, k_y) are small compared to k.

Meanwhile, in paraxial approximation $\theta \to 0$,

$$\hat{\mathrm{r}} = \sin\theta\cos\phi\,\hat{\mathrm{e}}_x + \sin\theta\sin\phi\,\hat{\mathrm{e}}_y + \cos\theta\,\hat{\mathrm{e}}_z \tag{1.20}$$

$$\approx \hat{\mathrm{e}}_z. \tag{1.21}$$

The Green function solution for a point emitter in free space can then be expanded to be

$$\frac{e^{i\mathrm{k}\cdot\mathrm{R}}}{R} \approx \frac{e^{ik_0(z-z')}}{z-z'} \exp\left[\frac{ik_0}{2(z-z')}\left|\mathrm{r}_\perp - \mathrm{r}'_\perp\right|\right], \tag{1.22}$$

where $\mathrm{R} = \mathbf{r} - \mathbf{r}'$. A far field from a point light emitter is usually paraxial approximation obedient.

1.3 Dipole oscillation and emission of polarized light

Here we present some results of electrical dipole radiations.

In Green's function language, we can obtain the electrical field as

$$\mathbf{E} = k^2 \int \mathbf{G}(\mathbf{r},\mathbf{r}')\mathbf{d}(\mathbf{r}')\mathrm{d}\mathbf{r}', \tag{1.23}$$

where $\mathbf{G}(\mathbf{r},\mathbf{r}')$ is the dyadic Green's functions for a dipole located at $\mathbf{r}'$ with a dipole momentum $\mathbf{d}(\mathbf{r}')$. $\mathbf{G}(\mathbf{r},\mathbf{r}')$ can be determined from the scalar Green's function $G_0(\mathbf{r},\mathbf{r}')$ by

$$\mathbf{G}(\mathbf{r},\mathbf{r}') = \left[\mathbf{I} + \frac{1}{k^2}\nabla\nabla\right] G_0(\mathbf{r},\mathbf{r}') \tag{1.24}$$

with the scalar Green's function I got in the last section given by

$$G_0(\mathbf{r},\mathbf{r}') = \frac{e^{ik|\mathbf{r}-\mathbf{r}'|}}{|\mathbf{r}-\mathbf{r}'|}. \tag{1.25}$$

To be continued: total dipole momentum and vacuum dipole momentum, more details on semi-classical and quantum model for the polarizability...

1.4 Light scattering without considering the mediation to the polarizability of the atom

To simplify the problem of light scattering in a nanofiber trapped atoms system, we treat the atoms as a dipole oscillator moving in a classical electrical field $\mathrm{E}_g(\mathbf{r},t)$ guided along the nanofiber, and re-emit a scattered optical field described by $\mathrm{E}^s(\mathbf{r},t)$ to interfere with the initial guided optical field. Formally, the total optical field $\mathrm{E}(\mathbf{r},t) = \mathrm{E}^g(\mathbf{r},t) + \mathrm{E}^s(\mathbf{r},t)$ implies a change of index of refraction and decoherence due to the presence of the atoms.

In the case of a nanofiber with a sub-wavelength radium, the high-order modes of the nanofiber can hardly be supported, which only leaves over the HE11 mode propagating along the nanofiber. Assuming the incident light is quasi-linearly polarized, the Cartesian components of the bound optical field are given, for $r_\perp > a$ (outside the fiber), by [1, 2]

$$\begin{aligned} E_x^g(r_\perp,\phi,z,t) &= A\frac{\beta_{11}J_1(h_{11}a)}{2q_{11}K_1(q_P11a)}[(1-s_{11})K_0(q_{11}r_\perp)\cos(\varphi_0) \\ &\quad + (1+s_{11})K_2(q_{11}r_\perp)\cos(2\phi-\varphi_0)]e^{-i(\omega t-f\beta_{11}z)}, \quad (1.26a) \\ E_y^g(r_\perp,\phi,z,t) &= A\frac{\beta_{11}J_1(h_{11}a)}{2q_{11}K_1(q_P11a)}[(1-s_{11})K_0(q_{11}r_\perp)\sin(\varphi_0) \\ &\quad + (1+s_{11})K_2(q_{11}r_\perp)\sin(2\phi-\varphi_0)]e^{-i(\omega t-f\beta_{11}z)}, \quad (1.26b) \\ E_z^g(r_\perp,\phi,z,t) &= iA\frac{J_1(h_{11}a)}{K_1(q_P11a)}K_1(q_{11}r_\perp)\cos(\phi-\varphi_0)e^{-i(\omega t-f\beta_{11}z)}, \quad (1.26c) \end{aligned}$$

and, for $r_\perp < a$ (inside the nanofiber), by

$$\begin{aligned} E_x^g(r_\perp,\phi,z,t) &= A\frac{\beta_{11}}{2h_{11}}[(1-s_{11})J_0(h_{11}r_\perp)\cos(\varphi_0) \\ &\quad - (1+s_{11})J_2(h_{11}r_\perp)\cos(2\phi-\varphi_0)]e^{-i(\omega t-f\beta_{11}z)}, \quad (1.27a) \\ E_y^g(r_\perp,\phi,z,t) &= A\frac{\beta_{11}}{2h_{11}}[(1-s_{11})J_0(h_{11}r_\perp)\sin(\varphi_0) \\ &\quad - (1+s_{11})J_2(h_{11}r_\perp)\sin(2\phi-\varphi_0)]e^{-i(\omega t-f\beta_{11}z)}, \quad (1.27b) \\ E_z^g(r_\perp,\phi,z,t) &= iAJ_1(h_{11}r)\cos(\phi-\varphi_0)e^{-i(\omega t-f\beta_{11}z)}, \quad (1.27c) \end{aligned}$$

with

$$\begin{aligned} s_{11} &= \left[\frac{1}{(h_{11}a)^2}+\frac{1}{(q_{11}a)^2}\right]\left[\frac{J_1'(h_{11}a)}{h_{11}aJ_1(h_{11}a)}+\frac{K_1'(q_{11}a)}{q_{11}aK_1(q_{11}a)}\right], \quad (1.28a) \\ h_{11} &= \sqrt{k_0^2n_1^2-\beta_{11}^2}, \quad (1.28b) \\ q_{11} &= \sqrt{\beta_{11}^2-k_0^2n_2^2}. \quad (1.28c) \end{aligned}$$

Here, k_0 is the vacuum wavenumber of the incident light; $f = +,-$ indicates forward or backward propagation direction; ϕ denotes the azimuthal angle in the transverse plane; φ_0 indicates the polarization axis for the incident polarization relative to the x axis; n_1 and n_2 are the refractive indices of inside and outside the nanofiber; β_{11} is the mode propagation constant; $1/h_{11}$ is the characteristic decay length for the bound mode inside the fiber; $1/q_{11}$ is the characteristic decay length outside the fiber; A is the real-valued amplitude for the linearly polarized input; J_l and K_l are the lth Bessel function of the first kind and the modified Bessel function of the second kind. As shown in Equs. 1.26 and 1.27, we can factorize the $\mathbf{E}^g(r_\perp, \phi, z, t)$ as $\mathbf{E}^g(r_\perp, \phi, z, t) = \boldsymbol{\mathcal{E}}^g(\mathbf{r})e^{i\omega t}$.

Alternatively, we can use the fundamental mode with rotating polarization to decompose arbitrary polarized mode propagating in the fiber. The solutions for the cylindrical components of the circulating polarized fundamental mode are given [1, 3], for $r_\perp < a$, by

$$E_{r_\perp}^{(\mu)}(r_\perp, \phi, z, t) = A\frac{\beta_{11}}{2h_{11}} \left[(1-s_{11})J_0(h_{11}r_\perp) - (1+s_{11})J_2(h_{11}r_\perp)\right]e^{-i(\omega t - f\beta_{11}z - p\phi)} \tag{1.29a}$$

$$E_{\phi}^{(\mu)}(r_\perp, \phi, z, t) = ipA\frac{\beta_{11}}{2h_{11}} \left[(1-s_{11})J_0(h_{11}r_\perp) + (1+s_{11})J_2(h_{11}r_\perp)\right]e^{-i(\omega t - f\beta_{11}z - p\phi)} \tag{1.29b}$$

$$E_{z}^{(\mu)}(r_\perp, \phi, z, t) = iAJ_1(h_{11}r_\perp)e^{-i(\omega t - f\beta_{11}z - p\phi)}, \tag{1.29c}$$

and, for $r_\perp > a$, by

$$E_{r_\perp}^{(\mu)}(r_\perp, \phi, z, t) = A\frac{\beta_{11}}{2h_{11}}\frac{J_1(h_{11}a)}{K_1(q_{11}a)} \left[(1-s_{11})K_0(q_{11}r_\perp) + (1+s_{11})K_2(q_{11}r_\perp)\right]e^{-i(\omega t - f\beta_{11}z - p\phi)} \tag{1.30a}$$

$$E_{\phi}^{(\mu)}(r_\perp, \phi, z, t) = ipA\frac{\beta_{11}}{2h_{11}}\frac{J_1(h_{11}a)}{K_1(q_{11}a)} \left[(1-s_{11})K_0(q_{11}r_\perp) - (1+s_{11})K_2(q_{11}r_\perp)\right]e^{-i(\omega t - f\beta_{11}z - p\phi)} \tag{1.30b}$$

$$E_{z}^{(\mu)}(r_\perp, \phi, z, t) = iA\frac{J_1(h_{11}a)}{K_1(q_{11}a)}K_1(q_{11}r_\perp)e^{-i(\omega t - f\beta_{11}z - p\phi)}. \tag{1.30c}$$

In Equs. 1.29 and 1.30, we denote the normalized bound fundamental modes as $\mathbf{E}^{(\mu)}(\mathbf{r}, t)$ by an index $\mu = (\omega, f, p)$, where $f = +, -$ denotes forward or backward propagation direction, and $p = +, -$ denotes the conterclockwise or clockwise of polarization. Similar to the qusi-linear case, we use $\boldsymbol{\mathcal{E}}^{p=\pm}$ to indicate the spatial components of the field with a given circulation pattern. For a linearly polarized HE11 mode, the cylindrical components are just the superposition of the two circular fields,

$$E_i^{lin} = \frac{1}{\sqrt{2}}(E_i^+ + E_i^-) \quad \text{or} \quad \mathcal{E}_i^{lin} = \frac{1}{\sqrt{2}}(\mathcal{E}_i^+ + \mathcal{E}_i^-), \quad i \in (r_\perp, \phi, z). \tag{1.31}$$

As discussed in Vetsch's dissertation [3], the real-valued amplitude factor A can be calculated by normalizing the total power of the light propagating in the fiber via the Poynting vector

$$\langle \mathbf{S} \rangle = \frac{1}{2} \Re \left[\boldsymbol{\mathcal{E}}^g(\mathbf{r}) \times \boldsymbol{\mathcal{H}}^g(\mathbf{r})^* \right], \tag{1.32}$$

where $\boldsymbol{\mathcal{H}}^g(\mathbf{r})$ is the magnetic field of the guided light. Since the z-component of the Poynting vector $\langle S_z \rangle$ qualifies the energy flux of the electromagnetic field in the propagation direction, integrating $\langle S_z \rangle$ over the transverse plane leads to the power propagating inside and outside the fiber

$$P_{in} = \int_0^{2\pi} \mathrm{d}\phi \int_0^a \langle S_z \rangle \, r_\perp \mathrm{d}r_\perp \tag{1.33}$$

$$P_{out} = \int_0^{2\pi} \mathrm{d}\phi \int_a^\infty \langle S_z \rangle \, r_\perp \mathrm{d}r_\perp. \tag{1.34}$$

Using the total transmission power $P = P_{in} + P_{out}$, the normalization constant A reads

$$A = \sqrt{\frac{4\mu_0 \omega P}{\pi a^2 \beta_{11}}} \left(D_{in} + D_{out} \right)^{-1/2}, \tag{1.35}$$

where

$$\begin{aligned} D_{in} = {} & (1 - s_{11}) \left[1 + (1 - s_{11}) \frac{\beta_{11}^2}{h_{11}^2} \right] \left(J_0^2(h_{11}a) + J_1^2(h_{11}a) \right) \\ & + (1 + s_{11}) \left[1 + (1 + s_{11}) \frac{\beta_{11}^2}{h_{11}^2} \right] \left(J_2^2(h_{11}a) - J_1(h_{11}a) J_3(h_{11}a) \right) \end{aligned} \tag{1.36}$$

$$\begin{aligned} D_{out} = {} & \frac{J_1^2(h_{11}a)}{K_1^2(q_{11}a)} \left\{ (1 - s_{11}) \left[1 - (1 - s_{11}) \frac{\beta_{11}^2}{q_{11}^2} \right] \left(K_0^2(q_{11}a) - K_1^2(q_{11}a) \right) \right. \\ & \left. + (1 + s_{11}) \left[1 - (1 + s_{11}) \frac{\beta_{11}^2}{q_{11}^2} \right] \left(K_2^2(q_{11}a) - K_1(q_{11}a) K_3(q_{11}a) \right) \right\}. \end{aligned} \tag{1.37}$$

As a first step, we only add one atom in the nanofiber-trapped-atoms system. Considering the detector is far away from the atom compared to the distance between the atom and the nanofiber, the paraxial approximation holds for our case where our measurement on the optical field is applied after a distant transmission through the fiber. We also assume that the emission from the atom propagates in free space by vanishing the boundary condition defined by the nanofiber, so that we can use the conclusion of the Green function for free space. The scattered optical field can be written as

$$\boldsymbol{\mathcal{E}}^s(\mathbf{r}) = -k_0^2 \left(\boldsymbol{\alpha} \cdot \boldsymbol{\mathcal{E}}^g(\mathbf{r}') \right)_\perp \frac{e^{ik_0 |\mathbf{r} - \mathbf{r}'|}}{|\mathbf{r} - \mathbf{r}'|} \tag{1.38}$$

$$= -k_0^2 \left[\boldsymbol{\alpha}\cdot\boldsymbol{\mathcal{E}}^g(\mathbf{r}') - (\hat{\mathrm{r}}\cdot\boldsymbol{\alpha}\cdot\boldsymbol{\mathcal{E}}^g(\mathbf{r}'))\,\hat{\mathrm{r}}\right] \frac{e^{ik_0|\mathbf{r}-\mathbf{r}'|}}{|\mathbf{r}-\mathbf{r}'|} \tag{1.39}$$

$$\approx -k_0^2 \left[\boldsymbol{\alpha}\cdot\boldsymbol{\mathcal{E}}^g(\mathbf{r}') - (\hat{\mathrm{e}}_z\cdot\boldsymbol{\alpha}\cdot\boldsymbol{\mathcal{E}}^g(\mathbf{r}'))\,\hat{\mathrm{e}}_z\right] \frac{e^{ik_0|\mathbf{r}-\mathbf{r}'|}}{|\mathbf{r}-\mathbf{r}'|} \tag{1.40}$$

$$= -k_0^2 \left[(\hat{\mathrm{e}}_{r_\perp}\cdot\boldsymbol{\alpha}\cdot\boldsymbol{\mathcal{E}}^g(\mathbf{r}'))\,\hat{\mathrm{e}}_{r_\perp} + (\hat{\mathrm{e}}_{\phi}\cdot\boldsymbol{\alpha}\cdot\boldsymbol{\mathcal{E}}^g(\mathbf{r}'))\,\hat{\mathrm{e}}_{\phi}\right] \frac{e^{ik_0|\mathbf{r}-\mathbf{r}'|}}{|\mathbf{r}-\mathbf{r}'|} \tag{1.41}$$

$$\approx \frac{-k_0^2 e^{ik_0(z-z')}}{z-z'} \left[(\hat{\mathrm{e}}_{r_\perp}\cdot\boldsymbol{\alpha}\cdot\boldsymbol{\mathcal{E}}^g(\mathbf{r}'))\,\hat{\mathrm{e}}_{r_\perp} + (\hat{\mathrm{e}}_{\phi}\cdot\boldsymbol{\alpha}\cdot\boldsymbol{\mathcal{E}}^g(\mathbf{r}'))\,\hat{\mathrm{e}}_{\phi}\right] \exp\left[\frac{ik_0\,|\mathrm{r}_\perp - \mathrm{r}'_\perp|}{2(z-z')}\right], \tag{1.42}$$

where $\boldsymbol{\alpha}$ is the polarizability tensor only depending on the internal state of the atom; $|\mathrm{r}_\perp - \mathrm{r}'_\perp| = \sqrt{r_\perp^2 + {r'_\perp}^2 - 2r_\perp r'_\perp \cos(\phi-\phi')}$ where $(r'_\perp, \phi', z')$ is the coordinate of the atom.

As shown in Equ. 1.42, the scattered field does not have a z-component in the far field by using a free space Green function.

We can decompose the guided mode into left- and right-handed circular fundamental modes using Equ. 1.31. For instance, if the incident light is x-polarized (horizontally polarized) with the normalized field $\boldsymbol{\mathcal{E}}^g(\mathbf{r}) = \boldsymbol{\mathcal{E}}_H(\mathbf{r})$, and $\mathbf{E}^g(\mathbf{r},t) = \boldsymbol{\mathcal{E}}_H(\mathbf{r})e^{-i\omega t}$ is a forward propagating light, we can use the relationship that

$$\boldsymbol{\mathcal{E}}^+ = \frac{1}{\sqrt{2}}\left(\boldsymbol{\mathcal{E}}_H + i\boldsymbol{\mathcal{E}}_V\right), \tag{1.43a}$$

$$\boldsymbol{\mathcal{E}}^- = \frac{1}{\sqrt{2}}\left(\boldsymbol{\mathcal{E}}_H - i\boldsymbol{\mathcal{E}}_V\right), \tag{1.43b}$$

where $\boldsymbol{\mathcal{E}}_V$ is the normalized mode with a y-polarized (vertically polarized) incident light which is orthogonal to $\boldsymbol{\mathcal{E}}_H$. Based on Equ. 1.43, we can solve for $\boldsymbol{\mathcal{E}}_H$ to give

$$\boldsymbol{\mathcal{E}}_H = \frac{1}{\sqrt{2}}\left(\boldsymbol{\mathcal{E}}^+ + \boldsymbol{\mathcal{E}}^-\right), \tag{1.44}$$

$$\boldsymbol{\mathcal{E}}_V = \frac{i}{\sqrt{2}}\left(\boldsymbol{\mathcal{E}}^- - \boldsymbol{\mathcal{E}}^+\right). \tag{1.45}$$

Therefore, the spatial dependent scattered electrical field can be given by

$$\boldsymbol{\mathcal{E}}^s(\mathbf{r}) \approx \frac{-k_0^2 e^{ik_0(z-z')}}{z-z'} \left[(\hat{\mathrm{e}}_{r_\perp}\cdot\boldsymbol{\alpha}\cdot\boldsymbol{\mathcal{E}}_H(\mathbf{r}'))\,\hat{\mathrm{e}}_{r_\perp} + (\hat{\mathrm{e}}_{\phi}\cdot\boldsymbol{\alpha}\cdot\boldsymbol{\mathcal{E}}_H(\mathbf{r}'))\,\hat{\mathrm{e}}_{\phi}\right] \exp\left[\frac{ik_0\,|\mathrm{r}_\perp - \mathrm{r}'_\perp|}{2(z-z')}\right] \tag{1.46}$$

$$\begin{aligned} &= -\frac{k_0^2 e^{ik_0(z-z')}}{\sqrt{2}(z-z')} \left(\hat{\mathrm{e}}_{r_\perp}\cdot\boldsymbol{\alpha}\cdot\left(\boldsymbol{\mathcal{E}}^+(\mathbf{r}') + \boldsymbol{\mathcal{E}}^-(\mathbf{r}')\right)\right)\hat{\mathrm{e}}_{r_\perp} \exp\left[\frac{ik_0\,|\mathrm{r}_\perp - \mathrm{r}'_\perp|}{2(z-z')}\right] \\ &\quad - \frac{k_0^2 e^{ik_0(z-z')}}{\sqrt{2}(z-z')} \left(\hat{\mathrm{e}}_{\phi}\cdot\boldsymbol{\alpha}\cdot\left(\boldsymbol{\mathcal{E}}^+(\mathbf{r}') + \boldsymbol{\mathcal{E}}^-(\mathbf{r}')\right)\right)\hat{\mathrm{e}}_{\phi} \exp\left[\frac{ik_0\,|\mathrm{r}_\perp - \mathrm{r}'_\perp|}{2(z-z')}\right]. \end{aligned} \tag{1.47}$$

Using Equs. 1.29 and 1.30, the $\boldsymbol{\mathcal{E}}_H(\mathbf{r}') = \boldsymbol{\mathcal{E}}^+(\mathbf{r}') + \boldsymbol{\mathcal{E}}^-(\mathbf{r}')$ is given by

$$\begin{aligned}
\mathcal{E}_{H r_\perp}(\mathbf{r}') &= A\frac{\beta_{11}}{h_{11}} \\
&\qquad [(1-s_{11})J_0(h_{11}r'_\perp) - (1+s_{11})J_2(h_{11}r'_\perp)]\, e^{if\beta_{11}z'} \cos\phi' && (1.48a) \\
\mathcal{E}_{H\phi}(\mathbf{r}') &= iA\frac{\beta_{11}}{2h_{11}} \\
&\qquad [(1-s_{11})J_0(h_{11}r'_\perp) + (1+s_{11})J_2(h_{11}r'_\perp)]\, e^{if\beta_{11}z'} \sin(\phi') && (1.48b) \\
\mathcal{E}_{Hz}(\mathbf{r}') &= i2AJ_1(h_{11}r'_\perp)e^{if\beta_{11}z'} \cos(\phi') && (1.48c)
\end{aligned}$$

for $r'_\perp < a$, and by

$$\begin{aligned}
\mathcal{E}_{H r_\perp}(\mathbf{r}') &= A\frac{\beta_{11}}{h_{11}}\frac{J_1(h_{11}a)}{K_1(q_{11}a)} \\
&\qquad [(1-s_{11})K_0(q_{11}r'_\perp) + (1+s_{11})K_2(q_{11}r'_\perp)]\, e^{if\beta_{11}z'} \cos(\phi') && (1.49a) \\
\mathcal{E}_{H\phi}(\mathbf{r}') &= iA\frac{\beta_{11}}{h_{11}}\frac{J_1(h_{11}a)}{K_1(q_{11}a)} \\
&\qquad [(1-s_{11})K_0(q_{11}r'_\perp) - (1+s_{11})K_2(q_{11}r'_\perp)]\, e^{if\beta_{11}z'} \sin(\phi') && (1.49b) \\
\mathcal{E}_{Hz}(\mathbf{r}') &= i2A\frac{J_1(h_{11}a)}{K_1(q_{11}a)}K_1(q_{11}r'_\perp)e^{if\beta_{11}z'} \cos(\phi') && (1.49c)
\end{aligned}$$

for $r'_\perp > a$. We define $\mathbf{T}^f(\mathbf{r}') = \boldsymbol{\alpha}\cdot \boldsymbol{\mathcal{E}}_H(\mathbf{r}') = \boldsymbol{\alpha}\cdot\left(\boldsymbol{\mathcal{E}}^+(\mathbf{r}') + \boldsymbol{\mathcal{E}}^-(\mathbf{r}')\right)$, which is a constant vector, and only the $r_\perp$ and ϕ components contribute to the scattered field in the far field. Now, Equ. 1.47 can be rewritten as

$$\boldsymbol{\mathcal{E}}^s(\mathbf{r}) = -\frac{k_0^2 e^{ik_0(z-z')}}{\sqrt{2}(z-z')} \exp\left[\frac{ik_0\,|\mathrm{r}_\perp - \mathrm{r}'_\perp|}{2(z-z')}\right]\left[T^f_{r_\perp}(\mathbf{r}')\hat{\mathrm{e}}_{r_\perp} + T^f_\phi(\mathbf{r}')\hat{\mathrm{e}}_\phi\right], \qquad (1.50)$$

where $T^f_{r_\perp}(\mathbf{r}')$ and $T^f_\phi(\mathbf{r}')$ are the $r_\perp$ and ϕ components of $\mathbf{T}^f(\mathbf{r}')$.

The total electrical field can be written as

$$\begin{aligned}
\boldsymbol{\mathcal{E}}(\mathbf{r}) &= \boldsymbol{\mathcal{E}}^g(\mathbf{r}) + \boldsymbol{\mathcal{E}}^s(\mathbf{r}) && (1.51) \\
&\approx \frac{1}{\sqrt{2}}\left(\boldsymbol{\mathcal{E}}^+(\mathbf{r}) + \boldsymbol{\mathcal{E}}^-(\mathbf{r})\right) \\
&\quad - \frac{k_0^2 e^{ik_0(z-z')}}{\sqrt{2}(z-z')}\left(\hat{\mathrm{e}}_{r_\perp}\cdot\boldsymbol{\alpha}\cdot\left(\boldsymbol{\mathcal{E}}^+(\mathbf{r}') + \boldsymbol{\mathcal{E}}^-(\mathbf{r}')\right)\right)\hat{\mathrm{e}}_{r_\perp} \exp\left[\frac{ik_0\,|\mathrm{r}_\perp - \mathrm{r}'_\perp|}{2(z-z')}\right] \\
&\quad - \frac{k_0^2 e^{ik_0(z-z')}}{\sqrt{2}(z-z')}\left(\hat{\mathrm{e}}_{\phi}\cdot\boldsymbol{\alpha}\cdot\left(\boldsymbol{\mathcal{E}}^+(\mathbf{r}') + \boldsymbol{\mathcal{E}}^-(\mathbf{r}')\right)\right)\hat{\mathrm{e}}_{\phi} \exp\left[\frac{ik_0\,|\mathrm{r}_\perp - \mathrm{r}'_\perp|}{2(z-z')}\right] && (1.52) \\
&= \frac{1}{\sqrt{2}}\boldsymbol{\mathcal{E}}_H(\mathbf{r}) - \frac{k_0^2 e^{ik_0(z-z')}}{\sqrt{2}(z-z')}\exp\left[\frac{ik_0|\mathrm{r}_\perp - \mathrm{r}'_\perp|}{2(z-z')}\right]\left[T^f_{r_\perp}(\mathbf{r}')\hat{\mathrm{e}}_{r_\perp} + T^f_\phi(\mathbf{r}')\hat{\mathrm{e}}_\phi\right]. && (1.53)
\end{aligned}$$

To further discuss how backward and forward scattering contribute to the bound mode, we consider both the space- and time-dependent electrical field of the scattered contribution $\mathbf{E}^s(\mathbf{r},t)$, and project it to the normalized forwarded and backwarded bound modes. In principle, we can decompose the scattered electrical field as

$$\mathbf{E}^s(\mathbf{r},t) = \sum_{\mu} C^{(\mu)}(z)\mathbf{E}^{(\mu)}(\mathbf{r},t), \tag{1.54}$$

with

$$C^{(\mu)}(z) = \int_0^{2\pi} \mathrm{d}\phi \int_0^{\infty} \mathbf{E}^{(\mu)^*}(\mathbf{r},t)\cdot\mathbf{E}^s(\mathbf{r},t) r_\perp \mathrm{d}r_\perp. \tag{1.55}$$

For the Green function we used above, the coefficients in the far field can be calculated as

$$\begin{aligned} C^{(\mu)}(z) = &-\frac{k_0^2 T^{f'}_{r_\perp}(\mathbf{r}') e^{ik_0(z-z')}}{\sqrt{2}(z-z')} \int_0^{2\pi} \mathrm{d}\phi \int_0^{\infty} \mathcal{E}^{(\mu)^*}_{r_\perp}(\mathbf{r}) \exp\left[\frac{ik_0\,|\mathrm{r}_\perp - \mathrm{r}'_\perp|}{2(z-z')}\right] r_\perp \mathrm{d}r_\perp \\ &-\frac{k_0^2 T^{f'}_{\phi}(\mathbf{r}') e^{ik_0(z-z')}}{\sqrt{2}(z-z')} \int_0^{2\pi} \mathrm{d}\phi \int_0^{\infty} \mathcal{E}^{(\mu)^*}_{\phi}(\mathbf{r}) \exp\left[\frac{ik_0\,|\mathrm{r}_\perp - \mathrm{r}'_\perp|}{2(z-z')}\right] r_\perp \mathrm{d}r_\perp \end{aligned} \tag{1.56}$$

$$\begin{aligned} = &-\frac{k_0^2 T^{f'}_{r_\perp}(\mathbf{r}') e^{ik_0(z-z')}}{\sqrt{2}(z-z')} \int_0^{2\pi} \mathrm{d}\phi \int_0^{a} \mathcal{E}^{(\mu)^*}_{r_\perp}(\mathbf{r}) \exp\left[\frac{ik_0\,|\mathrm{r}_\perp - \mathrm{r}'_\perp|}{2(z-z')}\right] r_\perp \mathrm{d}r_\perp \\ &-\frac{k_0^2 T^{f'}_{r_\perp}(\mathbf{r}') e^{ik_0(z-z')}}{\sqrt{2}(z-z')} \int_0^{2\pi} \mathrm{d}\phi \int_a^{\infty} \mathcal{E}^{(\mu)^*}_{r_\perp}(\mathbf{r}) \exp\left[\frac{ik_0\,|\mathrm{r}_\perp - \mathrm{r}'_\perp|}{2(z-z')}\right] r_\perp \mathrm{d}r_\perp \\ &-\frac{k_0^2 T^{f'}_{\phi}(\mathbf{r}') e^{ik_0(z-z')}}{\sqrt{2}(z-z')} \int_0^{2\pi} \mathrm{d}\phi \int_0^{a} \mathcal{E}^{(\mu)^*}_{\phi}(\mathbf{r}) \exp\left[\frac{ik_0\,|\mathrm{r}_\perp - \mathrm{r}'_\perp|}{2(z-z')}\right] r_\perp \mathrm{d}r_\perp \\ &-\frac{k_0^2 T^{f'}_{\phi}(\mathbf{r}') e^{ik_0(z-z')}}{\sqrt{2}(z-z')} \int_0^{2\pi} \mathrm{d}\phi \int_a^{\infty} \mathcal{E}^{(\mu)^*}_{\phi}(\mathbf{r}) \exp\left[\frac{ik_0\,|\mathrm{r}_\perp - \mathrm{r}'_\perp|}{2(z-z')}\right] r_\perp \mathrm{d}r_\perp \end{aligned} \tag{1.57}$$

$$\begin{aligned} = &-\frac{k_0^2 T^{f'}_{r_\perp}(\mathbf{r}') e^{ik_0(z-z')-if\beta_{11}z}}{\sqrt{2}(z-z')} \int_0^{2\pi} \mathrm{d}\phi \int_0^{a} \mathcal{E}^{(\mu)}_{r_\perp}(r_\perp) e^{-ip\phi} \exp\left[\frac{ik_0\,|\mathrm{r}_\perp - \mathrm{r}'_\perp|}{2(z-z')}\right] r_\perp \mathrm{d}r_\perp \\ &-\frac{k_0^2 T^{f'}_{r_\perp}(\mathbf{r}') e^{ik_0(z-z')-if\beta_{11}z}}{\sqrt{2}(z-z')} \int_0^{2\pi} \mathrm{d}\phi \int_a^{\infty} \mathcal{E}^{(\mu)}_{r_\perp}(r_\perp) e^{-ip\phi} \exp\left[\frac{ik_0\,|\mathrm{r}_\perp - \mathrm{r}'_\perp|}{2(z-z')}\right] r_\perp \mathrm{d}r_\perp \\ &-\frac{k_0^2 T^{f'}_{\phi}(\mathbf{r}') e^{ik_0(z-z')-if\beta_{11}z}}{\sqrt{2}(z-z')} \int_0^{2\pi} \mathrm{d}\phi \int_0^{a} \mathcal{E}^{(\mu)}_{\phi}(r_\perp) e^{-ip\phi} \exp\left[\frac{ik_0\,|\mathrm{r}_\perp - \mathrm{r}'_\perp|}{2(z-z')}\right] r_\perp \mathrm{d}r_\perp \\ &-\frac{k_0^2 T^{f'}_{\phi}(\mathbf{r}') e^{ik_0(z-z')-if\beta_{11}z}}{\sqrt{2}(z-z')} \int_0^{2\pi} \mathrm{d}\phi \int_a^{\infty} \mathcal{E}^{(\mu)}_{\phi}(r_\perp) e^{-ip\phi} \exp\left[\frac{ik_0\,|\mathrm{r}_\perp - \mathrm{r}'_\perp|}{2(z-z')}\right] r_\perp \mathrm{d}r_\perp \end{aligned} \tag{1.58}$$

$$
\begin{aligned}
&= -\frac{k_0^2 T_{r_\perp}^{f'}(\mathbf{r}')e^{ik_0(z-z')-if\beta_{11}z}}{\sqrt{2}(z-z')}\int_0^{2\pi}\mathrm{d}\phi\int_0^{a}\mathcal{E}_{r_\perp}^{(\mu)}(r_\perp)\exp\left[\frac{ik_0\,|\mathrm{r}_\perp-\mathrm{r}'_\perp|}{2(z-z')}-ip\phi\right]r_\perp\mathrm{d}r_\perp\\
&\quad-\frac{k_0^2 T_{r_\perp}^{f'}(\mathbf{r}')e^{ik_0(z-z')-if\beta_{11}z}}{\sqrt{2}(z-z')}\int_0^{2\pi}\mathrm{d}\phi\int_a^{\infty}\mathcal{E}_{r_\perp}^{(\mu)}(r_\perp)\exp\left[\frac{ik_0\,|\mathrm{r}_\perp-\mathrm{r}'_\perp|}{2(z-z')}-ip\phi\right]r_\perp\mathrm{d}r_\perp\\
&\quad-\frac{k_0^2 T_{\phi}^{f'}(\mathbf{r}')e^{ik_0(z-z')-if\beta_{11}z}}{\sqrt{2}(z-z')}\int_0^{2\pi}\mathrm{d}\phi\int_0^{a}\mathcal{E}_{\phi}^{(\mu)}(r_\perp)\exp\left[\frac{ik_0\,|\mathrm{r}_\perp-\mathrm{r}'_\perp|}{2(z-z')}-ip\phi\right]r_\perp\mathrm{d}r_\perp\\
&\quad-\frac{k_0^2 T_{\phi}^{f'}(\mathbf{r}')e^{ik_0(z-z')-if\beta_{11}z}}{\sqrt{2}(z-z')}\int_0^{2\pi}\mathrm{d}\phi\int_a^{\infty}\mathcal{E}_{\phi}^{(\mu)}(r_\perp)\exp\left[\frac{ik_0\,|\mathrm{r}_\perp-\mathrm{r}'_\perp|}{2(z-z')}-ip\phi\right]r_\perp\mathrm{d}r_\perp.
\end{aligned}
\tag{1.59}
$$

Using the relationship that $|\mathrm{r}_\perp-\mathrm{r}'_\perp|=\sqrt{r_\perp^2+r_\perp'^2-2r_\perp r'_\perp\cos(\phi-\phi')}$, the integral over ϕ can be separated as

$$
C_0^{(\mu)}(r_\perp,z)=\int_0^{2\pi}\mathrm{d}\phi\exp\left[\frac{ik_0\,|\mathrm{r}_\perp-\mathrm{r}'_\perp|}{2(z-z')}-ip\phi\right] \tag{1.60}
$$

$$
=\int_0^{2\pi}\mathrm{d}\phi\exp\left[\frac{ik_0\sqrt{r_\perp^2+r_\perp'^2-2r_\perp r'_\perp\cos(\phi-\phi')}}{2(z-z')}-ip\phi\right] \tag{1.61}
$$

$$
=\int_0^{2\pi}\mathrm{d}\phi\exp\left[\frac{ik_0\sqrt{r_\perp^2+r_\perp'^2}\sqrt{1-\frac{2r_\perp r'_\perp}{r_\perp^2+r_\perp'^2}\cos(\phi-\phi')}}{2(z-z')}-ip\phi\right]. \tag{1.62}
$$

Calculating this integration analytically is not trivial unless $r_\perp=r'_\perp$ or $\mathbf{r}_\perp$ parallel to $\mathbf{r}'_\perp$. We can calculate the projection coefficients numerically instead. Equ. 1.59 can be rewritten as

$$
C^{(\mu)}(z)=-\frac{k_0^2e^{ik_0(z-z')-if\beta_{11}z}}{\sqrt{2}(z-z')}\left[T_{r_\perp}^{f'}(\mathbf{r}')\mathcal{C}_{r_\perp}^{p}(z)+T_{\phi}^{f'}(\mathbf{r}')\mathcal{C}_{\phi}^{p}(z)\right] \tag{1.63}
$$

$$
=T_{r_\perp}^{f'}(\mathbf{r}')\mathcal{S}_{r_\perp}^{p}(z)+T_{\phi}^{f'}(\mathbf{r}')\mathcal{S}_{\phi}^{p}(z), \tag{1.64}
$$

where $\mathcal{C}_{r_\perp}^{p}(z)$ and $\mathcal{C}_{\phi}^{p}(z)$ correspond to the integrals with $\mathcal{E}_{r_\perp}^{(\mu)}$ and $\mathcal{E}_{\phi}^{(\mu)}$, repectively; Correspondingly, $\mathcal{S}_{r_\perp}^{p}(z)=\mathcal{A}(z)\mathcal{C}_{r_\perp}^{p}(z)$ and $\mathcal{S}_{\phi}^{p}(z)=\mathcal{A}(z)\mathcal{C}_{\phi}^{p}(z)$, where the interference factor

$$
\mathcal{A}(z)=-\frac{k_0^2e^{ik_0(z-z')-if\beta_{11}z}}{\sqrt{2}(z-z')}. \tag{1.65}
$$

We made $\mathbf{r}'=(r'_\perp,\phi',z')=(2a,0,0)$ and $\lambda_0=937.1$ nm, and numerically calculated the projection coefficients for the forward propagating and counterclockwise polarized fundamental mode. The results are shown in Figs 1.1 and 1.2. Notice that, due to numerical inaccuracy, there are some divergent integration noises for $z<5$ cm. As we can see from the figures, $\mathcal{A}(z)$ is a result of the interference of the point-scattered light and the bound mode, which decays as a function of $\frac{1}{z-z'}$ with a periodical phase change. The phase change should have a period of $2\pi/(k_0 - \beta_{11}) \sim \lambda_0$, where β_{11} is about one tenth of k_0. Due to limited computing resolution, the plots in Fig. 1.2 does not reflect the correct phase changing period. $\mathcal{C}^{(\mu)}(z)$ reflects how the scattered light synchronizes and better coupled with the bound mode as z increases. Combining these factors, the total projection factor $\mathcal{S}^{(\mu)}(z)$ decays dramatically when z is small as the $\frac{1}{z-z'}$ propagating decay dominates, and then increases with a periodical-like oscillation as the scattered light is close to a plane wave and can be well coupled and interfered with the bound mode. The beating frequency increases as the light propagates until it can be well coupled with the bound mode. Both $r_\perp$ and ϕ components of the projection coefficients have some difference as z is large.

Here are some phenomena needed to further explain: the different periods of changes for $r_\perp < a$ and $r_\perp > a$ cases; interference periods and beating periods are not as simple as normal interference model predicted (see Fig. 1.3)–this is because we used a rough resolution in z-direction to save computing time; the different behaviors of the two transverse components of the projection coefficients...

Technical problem: numerical integration does not work well for high oscillating functions. We need to artificially set up a very fine integrating x-axis to make it work properly. To fully solve this problem, we may need to consider better integration method, such as chebfun developed by Oxford (`http://www2.maths.ox.ac.uk/chebfun/`) which, I believe, is powerful to solve problems including definite integration, ordinary differential equations, contour integrals and roots finding.

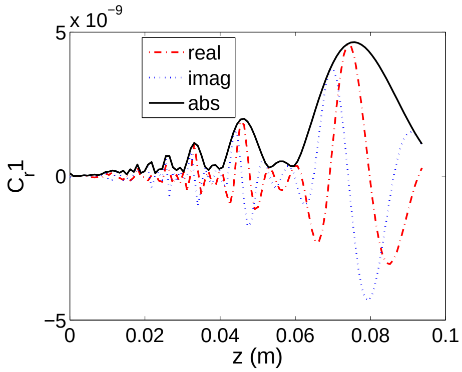

(a) $\mathcal{C}_{r_\perp}(z)$ for $r_\perp < a$

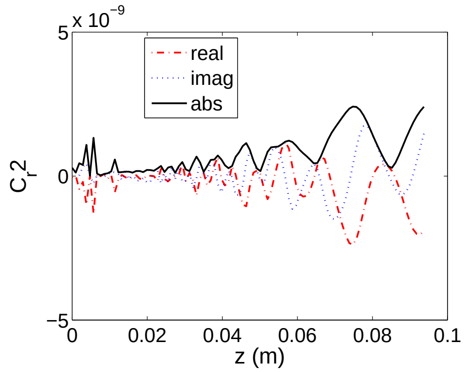

(b) $\mathcal{C}_{r_\perp}(z)$ for $r_\perp > a$

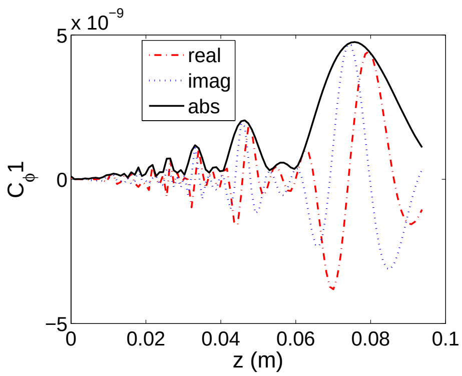

(c) $\mathcal{C}_{\phi}(z)$ for $r_\perp < a$

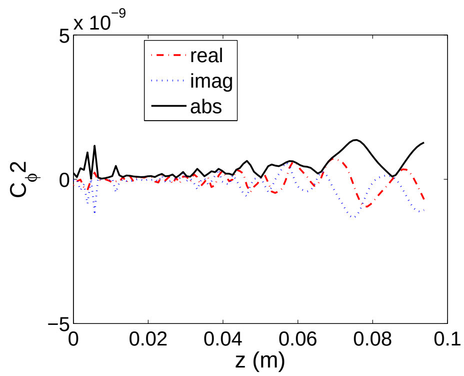

(d) $\mathcal{C}_{\phi}(z)$ for $r_\perp > a$

Figure 1.1: $\mathcal{C}^{(\omega,p=+,f=+)}(z)$. The values of these coefficients are in an arbitrary unit.

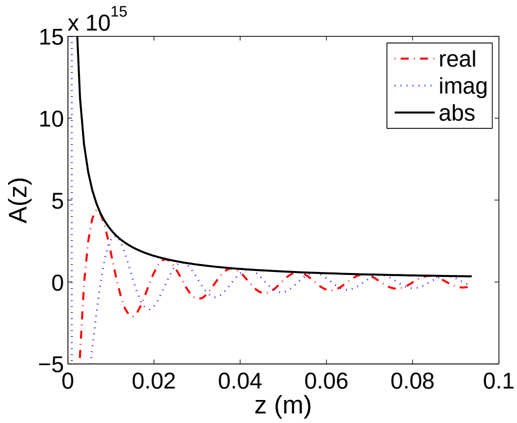

(a) $\mathcal{A}(z)$

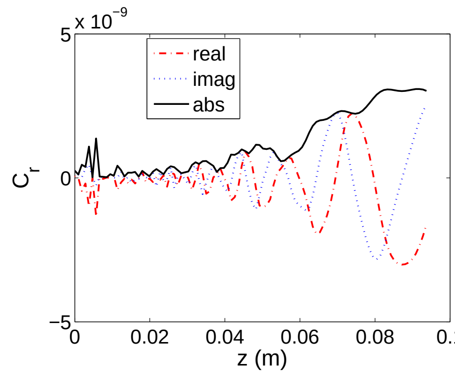

(b) $\mathcal{C}_{r_\perp}(z)$

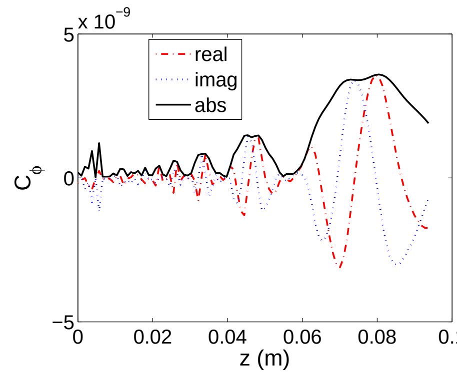

(c) $\mathcal{C}_\phi(z)$

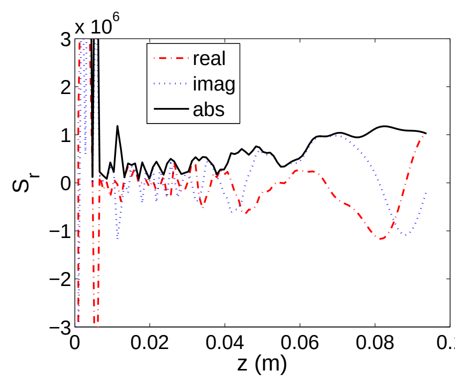

(d) $\mathcal{S}_{r_\perp}(z)$

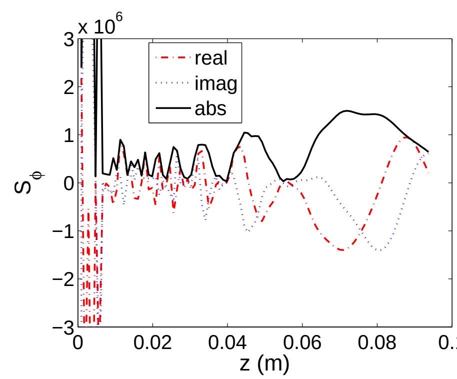

(e) $\mathcal{S}_\phi(z)$

Figure 1.2: $\mathcal{A}(z)$, $\mathcal{C}^{(\omega,p=+,f=+)}(z)$ and $\mathcal{S}^{(\omega,p=+,f=+)}(z)$. The values of these coefficients are in an arbitrary unit. There should be some fast chopping in $\mathcal{A}(z)$ and $\mathcal{S}^{(\mu)}(z)$. However, due to the cost of computing time, we did not give a fine enough calculation in our plots. See following plots for the calculation results with an improved resolution.

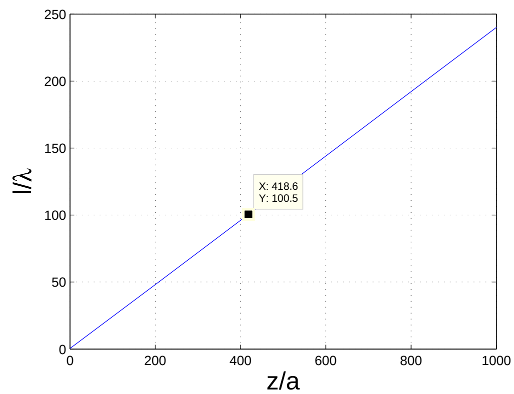

Figure 1.3: Wave path-difference of the interference between a monochromatic light emitted from a point atom located at $\mathbf{r}' = (r'_\perp, \phi', z') = (2a, 0, 0)$ and a laser beam propagating along the z-axis at the same wavelength $\lambda_0 = 937.1$ nm. The horizontal axis of the plot is scaled in terms of the radium a of the nanofiber. The vertical axis is the wave path-difference measured along the laser's propagation direction of z-axis, which is scaled by the wavelength $\lambda = \lambda_0$. As we can see, the interference period is uniform, and is on the order of $4.2a$. This rough calculation implies that the chopping frequency in z-direction should on the order of the wavelength, which should be reflected in Fig. 1.2 and related plots.

Notice that, calculation resolution matters to the results. For comparison, we run the exact simulation as above but with a better z-resolution. The results are shown in Figs. 1.4 and 1.5. In $z \in (0, 1)$ mm region, we calculate the coefficients in every 20 wavelengths; in $z \in [2, 100]$ mm region, we calculate the coefficients in every $\lesssim$ 1000 wavelengths. While in Figs. 1.1 and 1.2 before, we calculate the coefficients evenly in every 1000 wavelengths. Also, when we calculated the integrals in the figures below, we used a 3 times better resolution in $r_\perp \in (a, 5a)$ region, which gives more detailed features of the $\mathcal{C}^{(\mu)}(z)$ and $\mathcal{S}^{(\mu)}(z)$ plots. With this improved resolution, it takes more than one hour to run the full calculation on a Thinkpad X200 laptop.

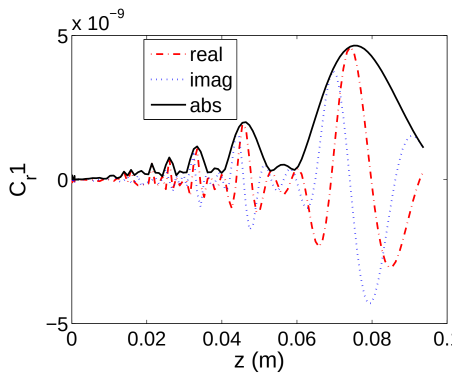

(a) $\mathcal{C}_{r_\perp}(z)$ for $r_\perp < a$

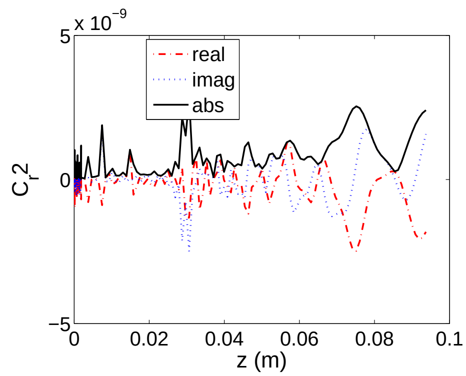

(b) $\mathcal{C}_{r_\perp}(z)$ for $r_\perp > a$

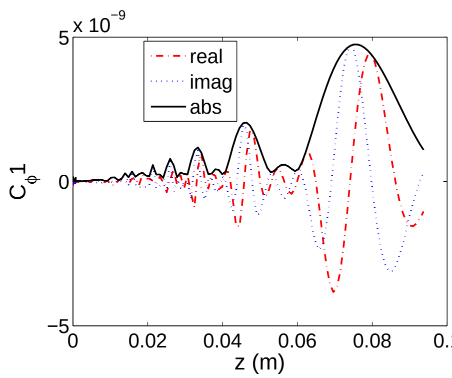

(c) $\mathcal{C}_{\phi}(z)$ for $r_\perp < a$

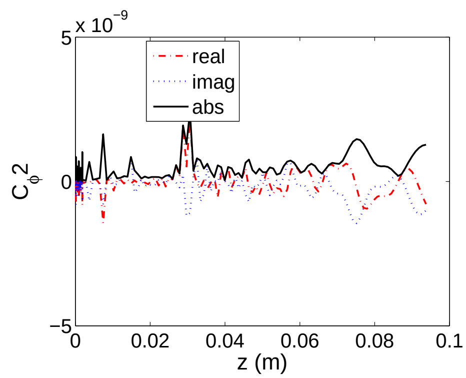

(d) $\mathcal{C}_{\phi}(z)$ for $r_\perp > a$

Figure 1.4: $\mathcal{C}^{(\omega,p=+,f=+)}(z)$. The values of these coefficients are in an arbitrary unit. Resolution is improved (see text).

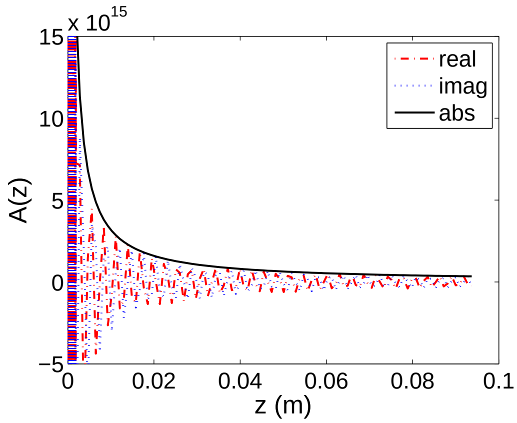

(a) $\mathcal{A}(z)$

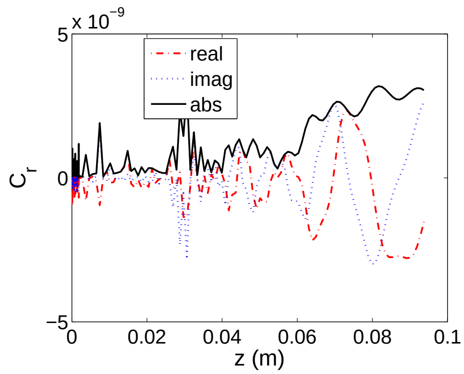

(b) $\mathcal{C}_{r_\perp}(z)$

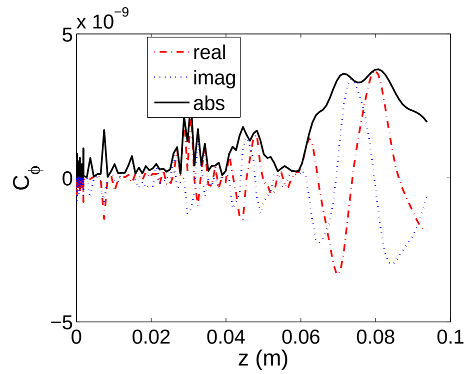

(c) $\mathcal{C}_{\phi}(z)$

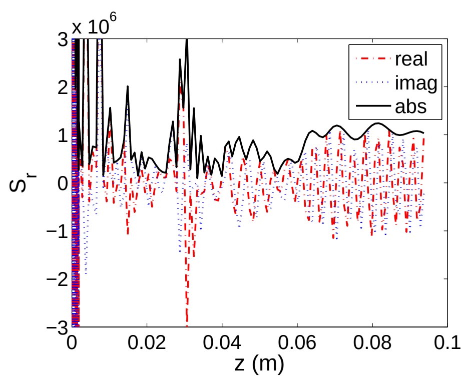

(d) $\mathcal{S}_{r_\perp}(z)$

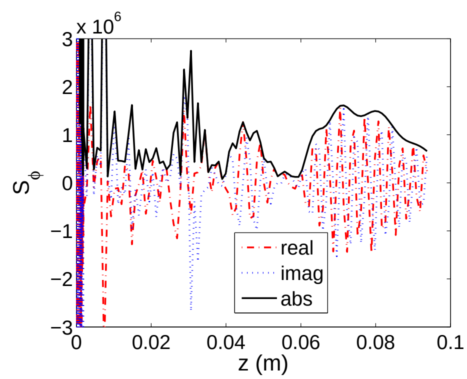

(e) $\mathcal{S}_{\phi}(z)$

Figure 1.5: $\mathcal{A}(z)$, $\mathcal{C}^{(\omega,p=+,f=+)}(z)$ and $\mathcal{S}^{(\omega,p=+,f=+)}(z)$. The values of these coefficients are in an arbitrary unit. Resolution is improved (see text).

1.5 Bound and radiation modes

In our study, it is critical to separate the bound mode and the radiation mode. In this section, we will go through a light propagation theory in the scenario of a nanofiber with a trapped atom.

Considering that the atom emits photons around the nanofiber, the total electrical field in our problem can be written as

$$\boldsymbol{\mathcal{E}}(\mathbf{r}) = \boldsymbol{\mathcal{E}}_{source}(\mathbf{r}) + \boldsymbol{\mathcal{E}}_{fiber}(\mathbf{r}) = \boldsymbol{\mathcal{E}}_{source}(\mathbf{r}) + \boldsymbol{\mathcal{E}}_{ref}(\mathbf{r}) + \boldsymbol{\mathcal{E}}_{tran}(\mathbf{r}), \tag{1.66}$$

where $\boldsymbol{\mathcal{E}}_{source}$ is the electrical field generated by the atom source; $\boldsymbol{\mathcal{E}}_{fiber}$ is the field due to the presence of the nanofiber, which includes the reflected electrical field $\boldsymbol{\mathcal{E}}_{ref}(\mathbf{r})$ (outside the nanofiber) and transmitted field $\boldsymbol{\mathcal{E}}_{tran}(\mathbf{r})$ (inside the nanofiber).

First, we only consider the light propagating in a nanofiber without any scatterers. We estimate the field propagating along the nanofiber is a cylindrical wave due to the geometrical symmetry of the nanofiber.

To fully calculate the electromagnetic field, we consider both electrical and magnetic fields, the spacial parts of which are governed by the wave equations

$$\left(\nabla^2 + k^2\varepsilon(\mathbf{r}_\perp)\right)\begin{pmatrix}\mathcal{E}_z(\mathbf{r})\\ \mathcal{B}_z(\mathbf{r})\end{pmatrix} = 0. \tag{1.67}$$

Notice that we are working in the cylindrical coordinate system, and only concentrate on the z-component of the fields, since all the other components can be expressed in terms of the z-components of the fields (see Appendix A.2. It will be discussed shortly).

We use an ansatz that

$$\mathcal{E}_z(r_\perp, \phi, z) = \psi(r_\perp, \phi)e^{i\beta z} \tag{1.68}$$

$$\mathcal{B}_z(r_\perp, \phi, z) = \zeta(r_\perp, \phi)e^{i\beta z}. \tag{1.69}$$

Substituting the above into Equ. 1.67, we obtain

$$\left(\nabla_\perp^2 + (k^2\varepsilon(\mathbf{r}_\perp) - \beta^2)\right)\begin{pmatrix}\psi(r_\perp, \phi)\\ \zeta(r_\perp, \phi)\end{pmatrix} = 0. \tag{1.70}$$

Now, the problem of solving a three dimensional wave equation for $\mathcal{E}(r_\perp, \phi, z)$ and $\mathcal{B}(r_\perp, \phi, z)$ turns into a problem of solving a two dimensional differential (mode) equation for $\psi(r_\perp, \phi)$ and $\zeta(r_\perp, \phi)$.

There are two special cases for the modes, in general. If $\psi = 0$ as a constant, which means there is no z-component of the electrical field, then the propagating mode is call a TE mode. Similarly, if $\zeta = 0$ as a constant, which corresponds to zero magnetic z-component, then this mode is called a TM mode. However, the modes in a waveguide with cylindrical symmetry cannot be grouped into TE and TM guided waves. In general, the modes with both electrical and magnetic nonzero z-components are known as EH and HE hybrid modes [4].

We focus on the electrical part for now. The magnetic field can be solved similarly. Equ. 1.70 gives

$$[\nabla_\perp^2 + k^2\varepsilon(r_\perp)]\psi(r_\perp, \phi) = \beta^2\psi(r_\perp, \phi). \tag{1.71}$$

Compared to the time-independent Schrodinger equation

$$\left[\frac{\hat{P}^2}{2m} + V(\hat{\mathbf{r}}_\perp)\right]\psi(\mathbf{r}_\perp) = E\psi(\mathbf{r}_\perp) \tag{1.72}$$

$$\text{or} \quad \left[\nabla_\perp^2 - V(r_\perp)\right]\psi(r_\perp, \phi) = -E\psi(r_\perp, \phi), \tag{1.73}$$

we can conclude that the mode equation (Equ. 1.71) is basically an eigenvalue equation if we make

$$V_{eff} = -k^2\varepsilon(\mathbf{r}_\perp) \sim V(\mathbf{r}_\perp) \tag{1.74}$$

$$-\beta^2 \sim E. \tag{1.75}$$

With these analogies, we can apply the method of distinguishing bound and unbound or radiative wave functions we used in the time-independent Schrodinger equation to distinguishing the bound and radiation modes in our nanofiber model.

In the time-independent Schrodinger problem, if $0 < E \leq V$, then the wave is bounded; if $E > V$, then the wave is unbounded. For the fiber mode, similarly, we can also use the relative position of V_{eff} and $-\beta^2$ to classify the bound and radiation modes (see Fig. 1.6).

Using the relationship that

$$\nabla^2{}_\perp = \frac{1}{r_\perp}\frac{\partial}{\partial r_\perp}\left(r_\perp\frac{\partial}{\partial r_\perp}\right) + \frac{1}{r_\perp^2}\frac{\partial^2}{\partial\phi^2}, \tag{1.76}$$

and the symmetry of the fiber, we can separate the mode function by

$$\psi(r_\perp, \phi) = \mathcal{E}_{z,\beta m}(r_\perp)e^{im\phi}, \tag{1.77}$$

and hence

$$\mathcal{E}_z(r_\perp, \phi, z) = \mathcal{E}_{z,\beta m}(r_\perp)e^{i(m\phi+\beta z)}, \tag{1.78}$$

where $\mathcal{E}_{z,\beta m}(r_\perp)$ satisfies the Bessel's equation

$$\left[\frac{\partial^2}{\partial {r_\perp}^2} + \frac{1}{r_\perp}\frac{\partial}{\partial r_\perp} - \frac{m^2}{r^2{}_\perp} + (k^2\varepsilon(r_\perp) - \beta^2)\right]\mathcal{E}_{z,\beta m}(r_\perp) = 0 \tag{1.79}$$

with

$$\varepsilon(r_\perp) = \begin{cases} 1, & r_\perp > a \\ \varepsilon_f, & r_\perp \leq a. \end{cases} \tag{1.80}$$

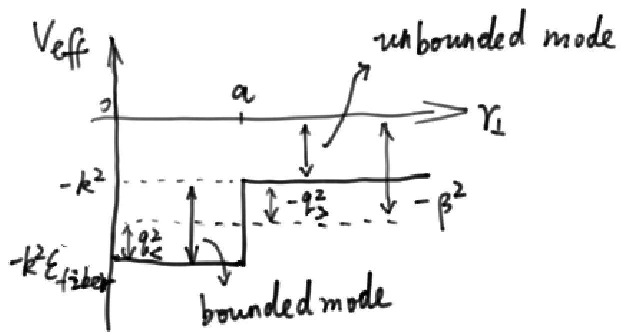

Figure 1.6: Bound and unbound states for the nanofiber eigenvalue problem. $\varepsilon(r_\perp) = \varepsilon_f = n_1^2$ if $r_\perp < a$; otherwise, $\varepsilon(r_\perp) = 1$. The parameter a is the radium of the nanofiber.

The general solution for $\mathcal{E}_{z,\beta m}(r_\perp)$ can be given in three cases corresponding to different boundary conditions

$$\mathcal{E}_{z,\beta m}(r_\perp) = \begin{cases} AJ_m(qr_\perp) + BY_m(qr_\perp) & \rightarrow J_m(\theta) \sim \cos\theta,\, Y_m(\theta) \sim \sin\theta. \\ CI_m(qr_\perp) + DK_m(qr_\perp) & \rightarrow I_m(\theta) \sim e^{\theta},\, K_m(\theta) \sim e^{-\theta}. \\ EH_m^{(1)}(qr_\perp) + FH_m^{(2)}(qr_\perp) & \rightarrow H_m^{(1)}(\theta) \sim e^{i\theta},\, H_m^{(2)}(\theta) \sim e^{-i\theta}. \end{cases} \tag{1.81}$$

The positive parameter $1/q$ is the characteristic decay length corresponding to $1/h_{11}$ and $1/q_{11}$ in the HE_{11} mode expression. Using the symmetric and convergent condition at $r_\perp = 0$ and ∞, as for bound modes, for example, if $k < \beta \leq k\sqrt{\varepsilon_f}$,

$$\begin{cases} r_\perp \leq a, & \mathcal{E}_{z,\beta m}(r_\perp) = AJ_m(hr_\perp), \quad h = \sqrt{k^2\varepsilon_f - \beta^2} > 0; \\ r_\perp > a, & \mathcal{E}_{z,\beta m}(r_\perp) = DK_m(qr_\perp), \quad q = \sqrt{\beta^2 - k^2} > 0. \end{cases} \tag{1.82}$$

Both β and h are discrete for bound modes. For scattered modes, $0 \leq \beta < k$, similarly,

$$\begin{cases} r_\perp \leq a, & \mathcal{E}_{z,\beta m}(r_\perp) = AJ_m(hr_\perp), \quad h = \sqrt{k^2\varepsilon_f - \beta^2} > 0; \\ r_\perp > a, & \mathcal{E}_{z,\beta m}(r_\perp) = EH_m^{(1)}(pr_\perp), \quad p = \sqrt{k^2 - \beta^2} > 0. \end{cases} \tag{1.83}$$

Both β and p are continuous. (Double check the general solutions and the consistence with Equ. 1.88.)

If β is a pure imaginary number, the field will have an exponential decay amplitude on z-direction, and will spread the energy away from the fiber axis. Reference [4] denotes the modes with pure imaginary β as evanescent modes. If β has both real and imaginary parts, the modes are denoted as leaky modes, which are combinations of radiation modes and evanescent modes. Except for the case that the incident light is highly directed at the complementary critical angle θ_c of geometric optics, only the radiation modes part can propagate for a long distance along the fiber axis. In our nanofiber system, we only consider the bound and radiation modes. The ranges of some waveguide parameters are given in Table 1.1. In the table, we have defined the normalized wave number[4], or V-number of a fiber as $V = k_f a\mathrm{NA}$. Here $k_f = \frac{2\pi}{\lambda}$, is the free space wave number, a is the radius of the core of the fiber, and NA is the numerical aperture of the fiber, $\mathrm{NA} = (n_{core}^2 - n_{cladding}^2)^{1/2} = n_{core}(2\Delta)^{1/2}$, with profile height parameter $\Delta = \frac{1}{2}(1 - n_{cladding}^2/n_{core}^2) \approx (n_{core} - n_{cladding})/n_{core}$. For different modes labeled with j, we always have $V_j^2 = a^2(h_j^2 + q_j^2)$ and $\lambda\beta_j/2\pi$ is a mode invariance. The TE and TM modes have non-vanishing cut-off frequencies, as $a \to 0$. The cutoff frequency is found from $V = a\omega(\Delta)^{1/2}/c = 2.405$ for silicon fiber. Only the lowest HE mode, HE_{11}, has no cutoff frequency as $a \to 0$. For $0 < V < 2.405$, which is the case of the nanofiber we are studying, it is the only mode that propagates in the fiber. For fixed ε_f, in the range that $0 \leq \beta \leq k\sqrt{\varepsilon_f}$, we can distinguish the radiative and bound mode as follows:

$$\begin{cases} 0 \leq \beta < k, & \to \textit{unbounded radiative modes;} \\ k < \beta \leq k\sqrt{\varepsilon_f}, & \to \exists a,\ \textit{HE}_{11} \textit{ is the only bound mode.} \end{cases} \tag{1.84}$$

Table 1.1: Ranges of fiber parameters for basic modes. Superscripts r and i denote real and imaginary parts. Subscripts j denotes the discrete values for bound modes. Adapted from Ref.[4] P.P.516 Table 25-1.

	β	h	p
Bound modes	$k < \beta_j \leq k\sqrt{\varepsilon_f}$	$0 \leq h_j < V/a$	$p_j^r = 0,\ p_j^i > 0$
Radiation modes	$0 \leq \beta < k$	$V/a < h \leq k\sqrt{\varepsilon_f}$	$0 < p \leq k$
Evanescent modes	$\beta^r = 0,\ \beta^i > 0$	$k\sqrt{\varepsilon_f} < h$	$k < p$

Due to the symmetry of equations, we also have

$$\mathcal{B}_z(r_\perp, \phi, z) = \mathcal{B}_{z,\beta m}(r_\perp)e^{i(m\phi+\beta z)}, \tag{1.85}$$

where $\mathcal{B}_{z,\beta m}(r_\perp)$ satisfies the same Bessel's equation as above.

Next, we consider the case that an atom–which can be treated as a dipole–is placed next to the nanofiber. Equ. 1.66 can be rewritten as

$$\boldsymbol{\mathcal{E}}(\mathbf{r}) = \boldsymbol{\mathcal{E}}_{source}(\mathbf{r}) + \boldsymbol{\mathcal{E}}_{ref}(\mathbf{r}) + \boldsymbol{\mathcal{E}}_{tran}(\mathbf{r}) \tag{1.86}$$

$$= \begin{cases} \boldsymbol{\mathcal{E}}_{dipole}(\mathbf{r}) + \boldsymbol{\mathcal{E}}_{ref}(\mathbf{r}) & r_\perp \geq a, \\ \boldsymbol{\mathcal{E}}_{tran}(\mathbf{r}) & r_\perp < a. \end{cases} \tag{1.87}$$

For longitudinal components of the electrical and magnetic fields we expand them as follows

$$\mathcal{E}_z^{(T)} = \sum_{m=-\infty}^{\infty} \int \mathrm{d}\beta e^{im(\phi-\phi')+i\beta(z-z')} \mathcal{E}_{z,m\beta}^{(T)}(r_\perp) \tag{1.88a}$$

$$= \sum_{m=-\infty}^{\infty} \int \mathrm{d}\beta e^{im(\phi-\phi')+i\beta(z-z')} c_{m\beta} J_m(hr_\perp), \tag{1.88b}$$

$$\mathcal{E}_z^{(0)} = \sum_{m=-\infty}^{\infty} \int \mathrm{d}\beta e^{im(\phi-\phi')+i\beta(z-z')} \mathcal{E}_{z,m\beta}^{(0)}(r_\perp) \tag{1.88c}$$

$$\mathcal{E}_z^{(R)} = \sum_{m=-\infty}^{\infty} \int \mathrm{d}\beta e^{im(\phi-\phi')+i\beta(z-z')} \mathcal{E}_{z,m\beta}^{(R)}(r_\perp) \tag{1.88d}$$

$$= \sum_{m=-\infty}^{\infty} \int \mathrm{d}\beta e^{im(\phi-\phi')+i\beta(z-z')} a_{m\beta} H_m^{(1)}(pr_\perp), \tag{1.88e}$$

$$\mathcal{B}_z^{(T)} = \sum_{m=-\infty}^{\infty} \int \mathrm{d}\beta e^{im(\phi-\phi')+i\beta(z-z')} \mathcal{B}_{z,m\beta}^{(T)}(r_\perp) \tag{1.89a}$$

$$= \sum_{m=-\infty}^{\infty} \int \mathrm{d}\beta e^{im(\phi-\phi')+i\beta(z-z')} d_{m\beta} J_m(hr_\perp), \tag{1.89b}$$

$$\mathcal{B}_z^{(0)} = \sum_{m=-\infty}^{\infty} \int \mathrm{d}\beta e^{im(\phi-\phi')+i\beta(z-z')} \mathcal{B}_{z,m\beta}^{(0)}(r_\perp) \tag{1.89c}$$

$$\mathcal{B}_z^{(R)} = \sum_{m=-\infty}^{\infty} \int \mathrm{d}\beta e^{im(\phi-\phi')+i\beta(z-z')} \mathcal{B}_{z,m\beta}^{(R)}(r_\perp) \tag{1.89d}$$

$$= \sum_{m=-\infty}^{\infty} \int \mathrm{d}\beta e^{im(\phi-\phi')+i\beta(z-z')} b_{m\beta} H_m^{(1)}(pr_\perp), \tag{1.89e}$$

where the subscripts indicate the field components of reflection (R), dipole oscillation in free space (0) and transmission (T). Notice that we have chosen $m = \pm 1$, as the nanofiber can only support HE_{11} modes. The $r_\perp$ and ϕ components of the fields can be obtained using Equ. A.10 and $\mathcal{B} = \mathcal{H}$ in Gauss units for given m. Also notice, whether we should use $e^{im\phi+i\beta z}$ or $e^{im(\phi-\phi')+i\beta(z-z')}$ in the equations above is not clear. Using $e^{im(\phi-\phi')+i\beta(z-z')}$ is more convenient to solve the boundary condition problem, but Klimov's paper uses the other one. See the discussion on boundary conditions next.

The free space dipole emits an electromagnetic field described by

$$\mathcal{A} = -ik\mathbf{d}_0 \frac{e^{ik|\mathbf{r}-\mathbf{r}'|}}{|\mathbf{r}-\mathbf{r}'|}, \tag{1.90}$$

$\mathcal{B}^{(0)} = \nabla \times \mathcal{A}$

$$
\begin{aligned}
&= -ik\nabla(\frac{e^{ik|\mathbf{r}-\mathbf{r}'|}}{|\mathbf{r}-\mathbf{r}'|})\times\mathbf{d}_0 = -ik\nabla G_0(\mathbf{r},\mathbf{r}')\times\mathbf{d}_0 \\
&= \left[\frac{d_z}{r_\perp}\frac{\partial G_0(\mathbf{r},\mathbf{r}')}{\partial\phi} - d_\phi\frac{\partial G_0(\mathbf{r},\mathbf{r}')}{\partial z}\right]\mathbf{e}_{r_\perp} \\
&\quad + \left[d_{r_\perp}\frac{\partial G_0(\mathbf{r},\mathbf{r}')}{\partial z} - d_z\frac{\partial G_0(\mathbf{r},\mathbf{r}')}{\partial r_\perp}\right]\mathbf{e}_\phi \\
&\quad + \left[d_\phi\frac{\partial G_0(\mathbf{r},\mathbf{r}')}{\partial r_\perp} - \frac{d_{r_\perp}}{r_\perp}\frac{\partial G_0(\mathbf{r},\mathbf{r}')}{\partial\phi}\right]\mathbf{e}_z \qquad (1.91) \\
&= \mathcal{B}^{(0)}_{r_\perp}\mathbf{e}_{r_\perp} + \mathcal{B}^{(0)}_\phi\mathbf{e}_\phi + \mathcal{B}^{(0)}_z\mathbf{e}_z, \qquad (1.92) \\
\mathcal{E}^{(0)} &= \frac{i}{k}\nabla\times\mathcal{H}^{(0)} = \frac{i}{k}\nabla\times\mathcal{B}^{(0)} \\
&= \frac{i}{k}(\frac{1}{r_\perp}\frac{\partial\mathcal{B}^{(0)}_z}{\partial\phi} - \frac{\partial\mathcal{B}^{(0)}_\phi}{\partial z})\mathbf{e}_{r_\perp} + \frac{i}{k}(\frac{\partial\mathcal{B}^{(0)}_{r_\perp}}{\partial z} - \frac{\partial\mathcal{B}^{(0)}_z}{\partial r_\perp})\mathbf{e}_\phi + \frac{i}{r_\perp k}(\frac{\partial(r_\perp\mathcal{B}^{(0)}_\phi)}{\partial r_\perp} - \frac{\partial\mathcal{B}^{(0)}_{r_\perp}}{\partial\phi})\mathbf{e}_z \\
&\qquad (1.93) \\
&= \mathcal{E}^{(0)}_{r_\perp}\mathbf{e}_{r_\perp} + \mathcal{E}^{(0)}_\phi\mathbf{e}_\phi + \mathcal{E}^{(0)}_z\mathbf{e}_z, \qquad (1.94)
\end{aligned}
$$

or, by Equ. (1.23). Here, $\mathbf{d}_0$ is the dipole momentum in vacuum. We denote $d_{r_\perp}$, d_ϕ and d_z as the cylindrical components of the dipole momentum at arbitrary observation point $\mathbf{r} = (r_\perp, \phi, z)$; while we use $d^0_{r_\perp}$, d^0_ϕ and d^0_z to indicate the cylindrical components of the dipole momentum at the dipole position $\mathbf{r}' = (r_\perp{}', \phi', z')$. As shown in Fig.(1.7) on page 24, we define the vector from the center of the nanofiber's core pointing to the atom position as x-axis, and the rotating symmetric axis of the nanofiber as the z-axis. The relationships between the dipole momentum components at $\mathbf{r}$ and $\mathbf{r}'$ can be given by

$$
\begin{aligned}
d_{r_\perp} &= \cos(\phi-\phi')d^0_{r_\perp} + \sin(\phi-\phi')d^0_\phi = \frac{1}{\sqrt{2}}\left(-e^{-i(\phi-\phi')}d_+ + e^{i(\phi-\phi')}d_-\right), \qquad (1.95) \\
d_\phi &= \cos(\phi-\phi')d^0_\phi - \sin(\phi-\phi')d^0_{r_\perp} = \frac{i}{\sqrt{2}}\left(e^{-i(\phi-\phi')}d_+ + e^{i(\phi-\phi')}d_-\right), \qquad (1.96) \\
d_z &= d^0_z, \qquad (1.97)
\end{aligned}
$$

where I have defined the position-independent reduced dipole vector components

$$
d_\pm \equiv \mp\frac{1}{\sqrt{2}}(d^0_{r_\perp} \pm i d^0_\phi). \qquad (1.98)
$$

The terms associated with $d_\pm$ in the dipole momentum formula lower or raise the mode index by 1. Notice that we have used $\phi-\phi'$ as the projected angle between $\mathbf{r}$ and $\mathbf{r}'$ to make the relationship work in general.

Using the expansion of the free-space dipole scalar Green function (Equ. (1.25))for the space $(r_\perp < r'_\perp)$ that

$$
G_0(\mathbf{r},\mathbf{r}') = \frac{e^{ik|\mathbf{r}-\mathbf{r}'|}}{|\mathbf{r}-\mathbf{r}'|}
$$

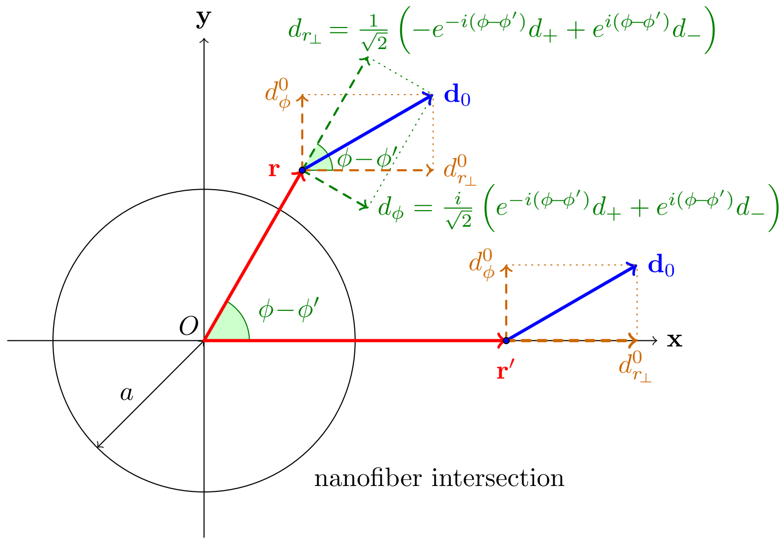

Figure 1.7: Dipole momentum decompositions in the xy-plane.

$$= \frac{i}{2}\sum_{m=-\infty}^{\infty}\oint_{C_1} \mathrm{d}\beta\, e^{im(\phi-\phi')+i\beta(z-z')} J_m(pr_\perp)\, H_m^{(1)}(pr'_\perp), \tag{1.99}$$

and for $(r_\perp > r'_\perp)$

$$G_0(\mathbf{r},\mathbf{r}') = \frac{e^{ik|\mathbf{r}-\mathbf{r}'|}}{|\mathbf{r}-\mathbf{r}'|}$$
$$= \frac{i}{2}\sum_{m=-\infty}^{\infty}\oint_{C_1} \mathrm{d}\beta\, e^{im(\phi-\phi')+i\beta(z-z')} J_m(pr'_\perp)\, H_m^{(1)}(pr_\perp), \tag{1.100}$$

one can obtain the free space dipole radiation field components in Equ. (1.88) and (1.89). The contour C_1 and field components can be found in Ref. [5].

The free radiation field components for the $r_\perp < r'_\perp$ region can be given by

$$\mathcal{B}_{z,m\beta}^{(0)} = \frac{k}{2r_\perp}\left[-id_{r_\perp} m H_m^{(1)}(pr'_\perp) J_m(pr_\perp) + d_\phi r_\perp H_m^{(1)}(pr'_\perp)\frac{\mathrm{d}}{\mathrm{d}r_\perp} J_m(pr_\perp)\right] \tag{1.101}$$

$$= \frac{k}{2}\left[\frac{-i}{r_\perp}\left(\cos(\phi-\phi')d_{r_\perp}^0 + \sin(\phi-\phi')d_\phi^0\right) m H_m^{(1)}(pr'_\perp) J_m(pr_\perp)\right.$$
$$\left. + \left(\cos(\phi-\phi')d_\phi^0 - \sin(\phi-\phi')d_{r_\perp}^0\right) H_m^{(1)}(pr'_\perp)\frac{\mathrm{d}}{\mathrm{d}r_\perp} J_m(pr_\perp)\right] \tag{1.102}$$

$$\mathcal{B}_{\phi,m\beta}^{(0)} = \frac{k}{2}\left[id_{r_\perp}\beta H_m^{(1)}(pr'_\perp)\, J_m(pr_\perp) - d_z H_m^{(1)}(pr'_\perp)\frac{\mathrm{d}}{\mathrm{d}r_\perp} J_m(pr_\perp)\right] \tag{1.103}$$

$$
\begin{aligned}
&= \frac{k}{2}\Bigg[i\left(\cos(\phi-\phi')d^0_{r_\perp}+\sin(\phi-\phi')d^0_\phi\right)\beta H^{(1)}_m\left(pr'_\perp\right)J_m\left(pr_\perp\right) \\
&\qquad -d^0_z H^{(1)}_m\left(pr'_\perp\right)\frac{\mathrm{d}}{\mathrm{d}r_\perp}J_m\left(pr_\perp\right)\Bigg] &(1.104)
\end{aligned}
$$

$$
\begin{aligned}
\mathcal{B}^{(0)}_{r_\perp,m\beta} &= \frac{k}{2}\left[\left(\frac{id_z m}{r_\perp}-id_\phi\beta\right)H^{(1)}_m\left(pr'_\perp\right)J_m\left(pr_\perp\right)\right] &(1.105)\\
&= \frac{k}{2}\Bigg[\left(\frac{id^0_z m}{r_\perp}-i\left(\cos(\phi-\phi')d^0_\phi-\sin(\phi-\phi')d^0_{r_\perp}\right)\beta\right) \\
&\qquad\qquad H^{(1)}_m\left(pr'_\perp\right)J_m\left(pr_\perp\right)\Bigg] &(1.106)
\end{aligned}
$$

$$
\begin{aligned}
\mathcal{E}^{(0)}_{z,m\beta} &= \frac{im}{2r_\perp}\left[\frac{d^0_z m}{r_\perp}+d^0_{r_\perp}\beta\sin(\phi-\phi')-d^0_\phi\beta\cos(\phi-\phi')\right]H^{(1)}_m\left(pr'_\perp\right)J_m\left(pr_\perp\right)\\
&\quad-\frac{1}{2}\left[d^0_{r_\perp}\beta\cos(\phi-\phi')+d^0_\phi\beta\sin(\phi-\phi')+\frac{id^0_z}{r_\perp}\right]H^{(1)}_m\left(pr'_\perp\right)\frac{\mathrm{d}}{\mathrm{d}r_\perp}J_m\left(pr_\perp\right)\\
&\quad-\frac{i}{2}d^0_z H^{(1)}_m\left(pr'_\perp\right)\frac{\mathrm{d}^2}{\mathrm{d}r^2_\perp}J_m\left(pr_\perp\right), &(1.107)
\end{aligned}
$$

$$
\begin{aligned}
\mathcal{E}^{(0)}_{\phi,m\beta} &= \frac{1}{2}\Bigg[d^0_{r_\perp}\left(\frac{m}{r^2_\perp}\cos(\phi-\phi')-i\beta^2\sin(\phi-\phi')\right)\\
&\qquad+d^0_\phi\left(\frac{m}{r^2_\perp}\sin(\phi-\phi')+i\beta^2\cos(\phi-\phi')\right)-\frac{id^0_z m\beta}{r_\perp}\Bigg]H^{(1)}_m(pr'_\perp)\,J_m(pr_\perp)\\
&\quad-\frac{m}{2r_\perp}\left(d^0_{r_\perp}\cos(\phi-\phi')+d^0_\phi\sin(\phi-\phi')\right)H^{(1)}_m\left(pr'_\perp\right)\frac{\mathrm{d}}{\mathrm{d}r_\perp}J_m\left(pr_\perp\right)\\
&\quad+\frac{i}{2}\left(d^0_{r_\perp}\sin(\phi-\phi')-d^0_\phi\cos(\phi-\phi')\right)H^{(1)}_m(pr'_\perp)\frac{\mathrm{d}^2}{\mathrm{d}r^2_\perp}J_m(pr_\perp), &(1.108)
\end{aligned}
$$

$$
\begin{aligned}
\mathcal{E}^{(0)}_{r_\perp,m\beta} &= \frac{1}{2}\Bigg\{d^0_{r_\perp}\left[\left(i\beta^2+\frac{im^2}{r^2_\perp}\right)\cos(\phi-\phi')-\frac{m}{r^2_\perp}\sin(\phi-\phi')\right]\\
&\qquad+d^0_\phi\left[\left(i\beta^2+\frac{im^2}{r^2_\perp}\right)\sin(\phi-\phi')+\frac{m}{r^2_\perp}\cos(\phi-\phi')\right]\Bigg\}H^{(1)}_m\left(pr'_\perp\right)J_m\left(pr_\perp\right)\\
&\quad-\frac{1}{2}\Bigg[\frac{d^0_{r_\perp}}{r_\perp}\left(i\cos(\phi-\phi')-m\sin(\phi-\phi')\right)\\
&\qquad+\frac{d^0_\phi}{r_\perp}\left(i\sin(\phi-\phi')+m\cos(\phi-\phi')\right)+d^0_z\beta\Bigg]H^{(1)}_m(pr'_\perp)\frac{\mathrm{d}}{\mathrm{d}r_\perp}J_m(pr_\perp)\,. &(1.109)
\end{aligned}
$$

More details on deriving the E-field components can be found in *Derivation of free-space E-field components.pdf.*

By exchanging J_m and $H^{(1)}_m$ functions, one can also obtain the field components that the reference [5] did not include for the case of $r_\perp > r'_\perp$. The magnetic and electrical fields components for $\mathbf{r}_\perp > \mathbf{r'}_\perp$ are

$$\mathcal{B}^{(0)}_{z,m\beta} = \frac{k}{2r_\perp}\left[-id_{r_\perp} m J_m(pr'_\perp) H^{(1)}_m(pr_\perp) + d_\phi r_\perp J_m(pr'_\perp)\frac{\mathrm{d}}{\mathrm{d}r_\perp} H^{(1)}_m(pr_\perp)\right] \tag{1.110}$$

$$= \frac{k}{2}\left[\frac{-i}{r_\perp}\left(\cos(\phi-\phi')d^0_{r_\perp} + \sin(\phi-\phi')d^0_\phi\right) m J_m(pr'_\perp) H^{(1)}_m(pr_\perp) + \left(\cos(\phi-\phi')d^0_\phi - \sin(\phi-\phi')d^0_{r_\perp}\right) J_m(pr'_\perp)\frac{\mathrm{d}}{\mathrm{d}r_\perp} H^{(1)}_m(pr_\perp)\right] \tag{1.111}$$

$$\mathcal{B}^{(0)}_{\phi,m\beta} = \frac{k}{2}\left[id_{r_\perp}\beta J_m\left(pr'_\perp\right) H^{(1)}_m\left(pr_\perp\right) - d_z J_m\left(pr'_\perp\right)\frac{\mathrm{d}}{\mathrm{d}r_\perp} H^{(1)}_m\left(pr_\perp\right)\right] \tag{1.112}$$

$$= \frac{k}{2}\left[i\left(\cos(\phi-\phi')d^0_{r_\perp} + \sin(\phi-\phi')d^0_\phi\right)\beta J_m\left(pr'_\perp\right) H^{(1)}_m\left(pr_\perp\right) - d^0_z J_m\left(pr'_\perp\right)\frac{\mathrm{d}}{\mathrm{d}r_\perp} H^{(1)}_m\left(pr_\perp\right)\right] \tag{1.113}$$

$$\mathcal{B}^{(0)}_{r_\perp,m\beta} = \frac{k}{2}\left[\left(\frac{id_z m}{r_\perp} - id_\phi\beta\right) J_m\left(pr'_\perp\right) H^{(1)}_m\left(pr_\perp\right)\right] \tag{1.114}$$

$$= \frac{k}{2}\left[\left(\frac{id^0_z m}{r_\perp} - i\left(\cos(\phi-\phi')d^0_\phi - \sin(\phi-\phi')d^0_{r_\perp}\right)\beta\right) J_m\left(pr'_\perp\right) H^{(1)}_m\left(pr_\perp\right)\right] \tag{1.115}$$

$$\begin{aligned}\mathcal{E}^{(0)}_{z,m\beta} = {} & \frac{im}{2r_\perp}\left[\frac{d^0_z m}{r_\perp} + d^0_{r_\perp}\beta\sin(\phi-\phi') - d^0_\phi\beta\cos(\phi-\phi')\right] J_m\left(pr'_\perp\right) H^{(1)}_m\left(pr_\perp\right)\\ & - \frac{1}{2}\left[d^0_{r_\perp}\beta\cos(\phi-\phi') + d^0_\phi\beta\sin(\phi-\phi') + \frac{id^0_z}{r_\perp}\right] J_m\left(pr'_\perp\right)\frac{\mathrm{d}}{\mathrm{d}r_\perp} H^{(1)}_m\left(pr_\perp\right)\\ & - \frac{i}{2} d^0_z J_m\left(pr'_\perp\right)\frac{\mathrm{d}^2}{\mathrm{d}r^2_\perp} H^{(1)}_m\left(pr_\perp\right),\end{aligned} \tag{1.116}$$

$$\begin{aligned}\mathcal{E}^{(0)}_{\phi,m\beta} = {} & \frac{1}{2}\left[d^0_{r_\perp}\left(\frac{m}{r^2_\perp}\cos(\phi-\phi') - i\beta^2\sin(\phi-\phi')\right)\right.\\ & \left. + d^0_\phi\left(\frac{m}{r^2_\perp}\sin(\phi-\phi') + i\beta^2\cos(\phi-\phi')\right) - \frac{id^0_z m\beta}{r_\perp}\right] J_m(pr'_\perp) H^{(1)}_m(pr_\perp)\\ & - \frac{m}{2r_\perp}\left(d^0_{r_\perp}\cos(\phi-\phi') + d^0_\phi\sin(\phi-\phi')\right) J_m\left(pr'_\perp\right)\frac{\mathrm{d}}{\mathrm{d}r_\perp} H^{(1)}_m\left(pr_\perp\right)\\ & + \frac{i}{2}\left(d^0_{r_\perp}\sin(\phi-\phi') - d^0_\phi\cos(\phi-\phi')\right) J_m(pr'_\perp)\frac{\mathrm{d}^2}{\mathrm{d}r^2_\perp} H^{(1)}_m(pr_\perp),\end{aligned} \tag{1.117}$$

$$\begin{aligned}\mathcal{E}^{(0)}_{r_\perp,m\beta} = {} & \frac{1}{2}\left\{d^0_{r_\perp}\left[\left(i\beta^2 + \frac{im^2}{r^2_\perp}\right)\cos(\phi-\phi') - \frac{m}{r^2_\perp}\sin(\phi-\phi')\right]\right.\\ & \left. + d^0_\phi\left[\left(i\beta^2 + \frac{im^2}{r^2_\perp}\right)\sin(\phi-\phi') + \frac{m}{r^2_\perp}\cos(\phi-\phi')\right]\right\} J_m\left(pr'_\perp\right) H^{(1)}_m\left(pr_\perp\right)\end{aligned}$$

$$
\begin{aligned}
&-\frac{1}{2}\left[\frac{d^0_{r_\perp}}{r_\perp}\left(i\cos(\phi-\phi')-m\sin(\phi-\phi')\right)\right.\\
&\qquad\left.+\frac{d^0_\phi}{r_\perp}\left(i\sin(\phi-\phi')+m\cos(\phi-\phi')\right)+d^0_z\beta\right]J_m(pr'_\perp)\frac{\mathrm{d}}{\mathrm{d}r_\perp}H^{(1)}_m(pr_\perp)\,.
\end{aligned}
\tag{1.118}
$$

By comparing the result with Klimov's paper for the $r_\perp < r'_\perp$ case, it seems Klimov and others had used some tricks, or they were more carefully to deal with the dipole orientations and components than we did here. By using the definitions of Bessel function to our expressions, all the second derivatives of Bessel functions can be transforming to zero- or first-order derivatives. The biggest difference between our expressions above and the results presented in the papers of Klimov and Nha [6] is that our expression of field components are ϕ-dependent while others are not. There are also $r'_\perp$'s on the denominators of Klimov's expressions, which may indicate that Klimov and colleagues might have used $r_\perp = r'_\perp$ case to build the general expression. Nha also used the dipole momentum components in Cartesian coordinate which shows only the reduced tensor components of the dipole momentum vectors matter to the field components.

By using the boundary conditions at $r_\perp = a$ and Equ. 1.87 that

$$
\mathcal{E}_z(r_\perp = a^>) = \mathcal{E}_z(r_\perp = a^<), \tag{1.119}
$$
$$
\mathcal{B}_z(r_\perp = a^>) = \mathcal{B}_z(r_\perp = a^<), \tag{1.120}
$$
$$
\mathcal{E}_\phi(r_\perp = a^>) = \mathcal{E}_\phi(r_\perp = a^<), \tag{1.121}
$$
$$
\mathcal{B}_\phi(r_\perp = a^>) = \mathcal{B}_\phi(r_\perp = a^<), \tag{1.122}
$$

where $a^<$ and $a^>$ denote the boundaries at the sides less and larger than a, and the connections between field components (Equ.(A.10)), we can obtain all unknown coefficients. In details, the boundary conditions yield

$$
a_{m\beta}H^{(1)}_m(pa) + \mathcal{E}^{(0)}_{z,m\beta}(r_\perp = a) = c_{m\beta}J_m(ha), \tag{1.123}
$$
$$
b_{m\beta}H^{(1)}_m(pa) + \mathcal{B}^{(0)}_{z,m\beta}(r_\perp = a) = d_{m\beta}J_m(ha), \tag{1.124}
$$
$$
\begin{aligned}
&\frac{m\beta}{p^2a}a_{m\beta}H^{(1)}_m(pa)+\frac{ik}{p^2}b_{m\beta}\left.\frac{\partial H^{(1)}_m(pr_\perp)}{\partial r_\perp}\right|_{r_\perp=a}-\mathcal{E}^{(0)}_{\phi,m\beta}(r_\perp=a)\\
&\qquad=\frac{m\beta}{h^2a}c_{m\beta}J_m(ha)+\frac{ik}{h^2}d_{m\beta}\left.\frac{\partial J_m(hr_\perp)}{\partial r_\perp}\right|_{r_\perp=a},
\end{aligned}
\tag{1.125}
$$
$$
\begin{aligned}
&\frac{m\beta}{p^2a}b_{m\beta}H^{(1)}_m(pa)+\frac{ik}{p^2}a_{m\beta}\left.\frac{\partial H^{(1)}_m(pr_\perp)}{\partial r_\perp}\right|_{r_\perp=a}+\mathcal{B}^{(0)}_{\phi,m\beta}(r_\perp=a)\\
&\qquad=\frac{m\beta}{h^2a}d_{m\beta}J_m(ha)+\frac{ik\varepsilon}{h^2}c_{m\beta}\left.\frac{\partial J_m(hr_\perp)}{\partial r_\perp}\right|_{r_\perp=a}.
\end{aligned}
\tag{1.126}
$$

One can substitute the first two equations into the last two equations, and obtain a equation set of $a_{m\beta}$ and $b_{m\beta}$ as below:

$$\begin{aligned}
&\left[\frac{m\beta}{p^2a}H_m^{(1)}(pa)-\frac{m\beta}{h^2a}H_m^{(1)}(pa)\right]a_{m\beta}\\
&+\left[\frac{ik}{p^2}\left.\frac{\partial H_m^{(1)}(pr_\perp)}{\partial r_\perp}\right|_{r_\perp=a}-\frac{ik}{h^2J_m(ha)}\left.\frac{\partial J_m(hr_\perp)}{\partial r_\perp}\right|_{r_\perp=a}H_m^{(1)}(pa)\right]b_{m\beta}\\
=&\frac{m\beta}{h^2a}\mathcal{E}_{z,m\beta}^{(0)}(r_\perp=a)+\frac{ik}{h^2J_m(ha)}\left.\frac{\partial J_m(hr_\perp)}{\partial r_\perp}\right|_{r_\perp=a}\mathcal{B}_{z,m\beta}^{(0)}(r_\perp=a)+\mathcal{E}_{\phi,m\beta}^{(0)}(r_\perp=a)
\end{aligned} \tag{1.127}$$

$$\begin{aligned}
&\left[\frac{m\beta}{p^2a}H_m^{(1)}(pa)-\frac{m\beta}{h^2a}H_m^{(1)}(pa)\right]b_{m\beta}\\
&+\left[\frac{ik}{p^2}\left.\frac{\partial H_m^{(1)}(pr_\perp)}{\partial r_\perp}\right|_{r_\perp=a}-\frac{ik\varepsilon}{h^2J_m(ha)}\left.\frac{\partial J_m(hr_\perp)}{\partial r_\perp}\right|_{r_\perp=a}H_m^{(1)}(pa)\right]a_{m\beta}\\
=&\frac{m\beta}{h^2a}\mathcal{B}_{z,m\beta}^{(0)}(r_\perp=a)+\frac{ik\varepsilon}{h^2J_m(ha)}\left.\frac{\partial J_m(hr_\perp)}{\partial r_\perp}\right|_{r_\perp=a}\mathcal{E}_{z,m\beta}^{(0)}(r_\perp=a)-\mathcal{B}_{\phi,m\beta}^{(0)}(r_\perp=a).
\end{aligned} \tag{1.128}$$

The solutions of $a_{m\beta}$ and $b_{m\beta}$ are given by Equs.(47-50) in Ref. [5]. We also have

$$c_{m\beta}=\frac{\mathcal{E}_{z,m\beta}^{(0)}(r_\perp=a)+H_m^{(1)}(pa)a_{m\beta}}{J_m(ha)}, \tag{1.129}$$

$$d_{m\beta}=\frac{\mathcal{H}_{z,m\beta}^{(0)}(r_\perp=a)+H_m^{(1)}(pa)b_{m\beta}}{J_m(ha)}. \tag{1.130}$$

Now, we only consider the $m=\pm1$ modes, and hence Equs. 1.88, 1.89 and the corresponding ϕ and $r_\perp$ components can be explicitly expressed as contour integrals as below

$$\mathcal{E}_z^{(T)}=\sum_{m=\pm1}\oint_{C_1}\mathrm{d}\beta e^{im(\phi-\phi')+i\beta(z-z')}c_{m\beta}J_m(hr_\perp), \tag{1.131a}$$

$$\mathcal{E}_z^{(0)}=\sum_{m=\pm1}\oint_{C_1}\mathrm{d}\beta e^{im(\phi-\phi')+i\beta(z-z')}\mathcal{E}_{z,m\beta}^{(0)}(r_\perp) \tag{1.131b}$$

$$\mathcal{E}_z^{(R)}=\sum_{m=\pm1}\oint_{C_1}\mathrm{d}\beta e^{im(\phi-\phi')+i\beta(z-z')}a_{m\beta}H_m^{(1)}(pr_\perp), \tag{1.131c}$$

$$\mathcal{B}_z^{(T)}=\sum_{m=\pm1}\oint_{C_1}\mathrm{d}\beta e^{im(\phi-\phi')+i\beta(z-z')}d_{m\beta}J_m(hr_\perp), \tag{1.132a}$$

$$\mathcal{B}_z^{(0)}=\sum_{m=\pm1}\oint_{C_1}\mathrm{d}\beta e^{im(\phi-\phi')+i\beta(z-z')}\mathcal{B}_{z,m\beta}^{(0)}(r_\perp) \tag{1.132b}$$

$$\mathcal{B}_z^{(R)} = \sum_{m=\pm 1} \oint_{C_1} \mathrm{d}\beta e^{im(\phi-\phi')+i\beta(z-z')} b_{m\beta} H_m^{(1)}(pr_\perp). \tag{1.132c}$$

To distinguish the bound and radiation modes contributions, one can use branch cuts and isolated poles to separate the contour integral along C_1. The bound modes are associated with poles, and hence can be represented as residues as below.

$$\mathcal{E}_z^{(T)} = 2\pi i \sum_{m=\pm 1} \sum_{\beta_{1,m=\pm 1}} \mathrm{Res}\left[e^{im(\phi-\phi')+i\beta(z-z')} c_{m\beta} J_m(hr_\perp)\right]_{\beta=\beta_{1,m}}, \tag{1.133a}$$

$$\mathcal{E}_z^{(0)} = 2\pi i \sum_{m=\pm 1} \sum_{\beta_{1,m=\pm 1}} \mathrm{Res}\left[e^{im(\phi-\phi')+i\beta(z-z')} \mathcal{E}_{z,m\beta}^{(0)}(r_\perp)\right]_{\beta=\beta_{1,m}}, \tag{1.133b}$$

$$\mathcal{E}_z^{(R)} = 2\pi i \sum_{m=\pm 1} \sum_{\beta_{1,m=\pm 1}} \mathrm{Res}\left[e^{im(\phi-\phi')+i\beta(z-z')} a_{m\beta} H_m^{(1)}(pr_\perp)\right]_{\beta=\beta_{1,m}}, \tag{1.133c}$$

$$\mathcal{B}_z^{(T)} = 2\pi i \sum_{m=\pm 1} \sum_{\beta_{1,m=\pm 1}} \mathrm{Res}\left[e^{im(\phi-\phi')+i\beta(z-z')} d_{m\beta} J_m(hr_\perp)\right]_{\beta=\beta_{1,m}}, \tag{1.134a}$$

$$\mathcal{B}_z^{(0)} = 2\pi i \sum_{m=\pm 1} \sum_{\beta_{1,m=\pm 1}} \mathrm{Res}\left[e^{im(\phi-\phi')+i\beta(z-z')} \mathcal{B}_{z,m\beta}^{(0)}(r_\perp)\right]_{\beta=\beta_{1,m}}, \tag{1.134b}$$

$$\mathcal{B}_z^{(R)} = 2\pi i \sum_{m=\pm 1} \sum_{\beta_{1,m=\pm 1}} \mathrm{Res}\left[e^{im(\phi-\phi')+i\beta(z-z')} b_{m\beta} H_m^{(1)}(pr_\perp)\right]_{\beta=\beta_{1,m}}. \tag{1.134c}$$

The radiation modes are associated with the branch cuts C_2 which is presented in Ref. [5].

$$\mathcal{E}_z^{(T)} = \sum_{m=\pm 1} \oint_{C_2} \mathrm{d}\beta e^{im(\phi-\phi')+i\beta(z-z')} c_{m\beta} J_m(hr_\perp), \tag{1.135a}$$

$$\mathcal{E}_z^{(0)} = \sum_{m=\pm 1} \oint_{C_2} \mathrm{d}\beta e^{im(\phi-\phi')+i\beta(z-z')} \mathcal{E}_{z,m\beta}^{(0)}(r_\perp), \tag{1.135b}$$

$$\mathcal{E}_z^{(R)} = \sum_{m=\pm 1} \oint_{C_2} \mathrm{d}\beta e^{im(\phi-\phi')+i\beta(z-z')} a_{m\beta} H_m^{(1)}(pr_\perp), \tag{1.135c}$$

$$\mathcal{B}_z^{(T)} = \sum_{m=\pm 1} \oint_{C_2} \mathrm{d}\beta e^{im(\phi-\phi')+i\beta(z-z')} d_{m\beta} J_m(hr_\perp), \tag{1.136a}$$

$$\mathcal{B}_z^{(0)} = \sum_{m=\pm 1} \oint_{C_2} \mathrm{d}\beta e^{im(\phi-\phi')+i\beta(z-z')} \mathcal{B}_{z,m\beta}^{(0)}(r_\perp), \tag{1.136b}$$

$$\mathcal{B}_z^{(R)} = \sum_{m=\pm 1} \oint_{C_2} \mathrm{d}\beta e^{im(\phi-\phi')+i\beta(z-z')} b_{m\beta} H_m^{(1)}(pr_\perp). \tag{1.136c}$$

One can obtain the bound and radiation field components with the dipole oriented in z, ϕ and $r_\perp$ directions by substituting the $\boldsymbol{\mathcal{E}}_{m\beta}^{(0)}(r_\perp)$ expressions for corresponding cases into Equs. 1.133, 1.134, 1.135 and 1.136.

To calculate the bound modes, we need to calculate the residues at isolated poles with $\beta_{1,m}$ and $m = \pm 1$. The poles can be found by using the condition that

$$D = P^2 + QR = 0, \tag{1.137}$$

or

$$\begin{aligned}
&\beta^2 m^2 k^4 \left(J_m(ha) H_m^{(1)}(pa)\right)^2 (\varepsilon_f - 1)^2 \\
&-h^2 p^2 a^2 k^2 \left(h J_m(ha) \frac{\mathrm{d}}{\mathrm{d}(pa)} H_m^{(1)}(pa) - p H_m^{(1)}(pa) \frac{\mathrm{d}}{\mathrm{d}(ha)} J_m(ha)\right) \\
&\left(h J_m(ha) \frac{\mathrm{d}}{\mathrm{d}(pa)} H_m^{(1)}(pa) - \varepsilon_f p H_m^{(1)}(pa) \frac{\mathrm{d}}{\mathrm{d}(ha)} J_m(ha)\right) = 0.
\end{aligned} \tag{1.138}$$

Here are some useful relationships to solve the equation above:

$$J_{-m}(z) = (-1)^n J_n(z), \quad H_{-m}^{(1)}(z) = e^{m\pi i} H_m^{(1)}(z), \tag{1.139}$$

$$\frac{\mathrm{d}}{\mathrm{d}z} J_m(z) = \frac{1}{2}\left(J_{m-1}(z) - J_{m+1}(z)\right), \tag{1.140}$$

$$\frac{\mathrm{d}}{\mathrm{d}z} H_m^{(1)}(z) = \frac{1}{2}\left(H_{m-1}^{(1)}(z) - H_{m+1}^{(1)}(z)\right). \tag{1.141}$$

We can rewrite Equ. 1.138 as

$$\begin{aligned}
&\beta^2 m^2 k^2 \left(J_m(ha) H_m^{(1)}(pa)\right)^2 (\varepsilon_f - 1)^2 \\
=&\frac{h^2 p^2 a^2}{4}\left[h J_m(ha)\left(H_{m-1}^{(1)}(pa) - H_{m+1}^{(1)}(pa)\right) - p H_m^{(1)}(pa)\left(J_{m-1}(ha) - J_{m+1}(ha)\right)\right] \\
&\left[h J_m(ha)\left(H_{m-1}^{(1)}(pa) - H_{m+1}^{(1)}(pa)\right) - \varepsilon_f p H_m^{(1)}(pa)\left(J_{m-1}(ha) - J_{m+1}(ha)\right)\right].
\end{aligned} \tag{1.142}$$

Since both h and p are functions of β, the equation above is complicated for solving β. If $ka < 0.8$, asymptotic approximation is good enough to solve Equ. 1.142 and give an analytical solution for β [5]. However, in our nanofiber case, the $ka < 0.8$ condition is not satisfied. We can only numerically solve Equ. 1.142 for β with $m = \pm 1$.

Numerical solutions and comparison with bare nanofiber eigenfunction... Numerically, they are the same.

Next, we can solve the bound modes by differentiating the functions inside of *Res* signs and inserting the values of $\beta_{1,m=\pm 1}$. (Q: are those poles all of order 1?) The transverse components of the fields can be obtained from the longitudinal components using the relations of Equ. A.10. Can be checked by reproducing the decay rates following Klimov's paper [5]...

To calculate the total decay rate of the atom with the enhancement due to the radiation, we need to find out the functions describing the branch cuts and the integration path for the radiation modes. The equation defining the branch cut is given by

$$\mathrm{Im}\,[p] = 0. \tag{1.143}$$

By setting $\beta = x + iy$, we can rewrite

$$p = \sqrt{k^2 - \beta^2} \tag{1.144}$$

$$= \left[(k^2 - x^2 + y^2)^2 + 4x^2y^2\right]^{1/4} e^{\frac{i}{2}\arctan\frac{-2xy}{k^2-x^2+y^2}}. \tag{1.145}$$

Hence Equ. 1.143 yields

$$0 = \left[(k^2 - x^2 + y^2)^2 + 4x^2y^2\right]^{1/4} \sin\left[\frac{1}{2}\arctan\frac{-2xy}{k^2 - x^2 + y^2}\right] \tag{1.146}$$

$$= \frac{1}{\sqrt{2}}\left[(k^2-x^2+y^2)^2+4x^2y^2\right]^{1/4}\sqrt{1-\cos\left(\arctan\frac{-2xy}{k^2-x^2+y^2}\right)} \tag{1.147}$$

$$= \frac{1}{\sqrt{2}}\left[(k^2-x^2+y^2)^2+4x^2y^2\right]^{1/4}\sqrt{1-\frac{k^2-x^2+y^2}{\left[(k^2-x^2+y^2)^2+4x^2y^2\right]^{1/2}}} \tag{1.148}$$

$$= \sqrt{\left[(k^2 - x^2 + y^2)^2 + 4x^2y^2\right]^{1/2} - (k^2 - x^2 + y^2)}, \tag{1.149}$$

which gives

$$\left[(k^2 - x^2 + y^2)^2 + 4x^2y^2\right]^{1/2} = (k^2 - x^2 + y^2), \tag{1.150}$$

$$\Leftrightarrow \qquad x^2y^2 = 0. \tag{1.151}$$

Obviously, the x-axis between $[-k, k]$ and the entire y-axis are the branch cuts. To separate the branches into upper and lower parts, we can define an arbitrary small positive number $\delta\epsilon \to 0$ so that Equ. 1.151 gives

$$xy = \delta\epsilon. \tag{1.152}$$

In this way, the branch cuts are symmetrically separated into top-right and lower-left parts. For the top-right branch, one can choose the integration path as shown in Fig. 1.8 to apply the contour integral detouring the branch cut.

In the case that the nanofiber can be treated as a lossless medium, the contour integral can be treated as an integral over real axis from 0 to k. Since there is a divergence problem as k, we are looking forward to simplify the integrand to see if the Hankel function can be canceled out at the limit of $\beta \to k$...

Also, working on simplify the residue calculation without doing any integral...

Pointing vectors and energy distribution...

Define transmitting and reflecting rates...

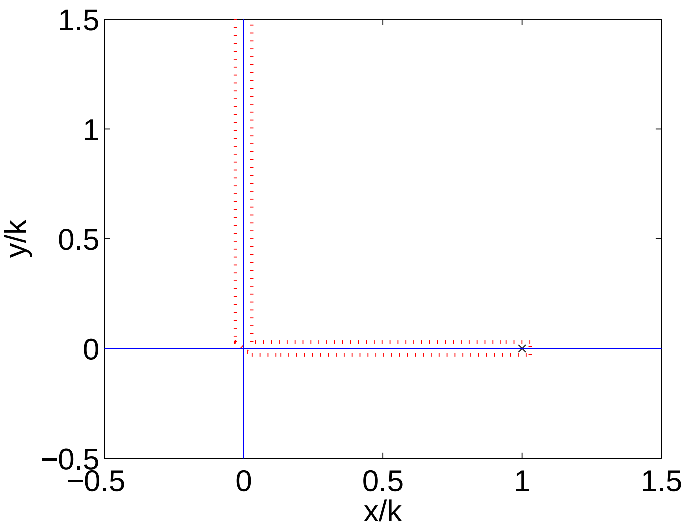

Figure 1.8: Integration path of the contour integral for radiation modes.

1.6 Bound and unbound modes of a nanofiber with a tilt incident plane wave

As an example of applying the technique we used above to solve the bound and unbound modes under cylindrical boundary conditions, below, we show an application on solving the nanofiber problem with a tilt incident plane wave.

The key to solve this kind of problems is to decompose all field functions into cylindrical functions. The bare nanofiber modes have already been decomposed into cylindrical functions in the last section; therefore, here, we only need to decompose the incident field as cylindrical functions.

We assume the incident plane wave is given by

$$\mathbf{E}(\mathbf{r}, t) = \Re\left[\mathbf{U}(\mathbf{r}, t)\right] = \mathbf{E}_0 \cos(\mathbf{k} \cdot \mathbf{r} - \omega t + \phi_0), \tag{1.153}$$

where the forward propagating wave can be given by

$$\mathbf{U}(\mathbf{r}, t) = \mathbf{U}_0 e^{i(\mathbf{k} \cdot \mathbf{r} - \omega t + \phi_0)} \tag{1.154}$$

$$= \mathbf{U}_0 e^{i\mathbf{k} \cdot \mathbf{r}} e^{i(\phi_0 - \omega t)}. \tag{1.155}$$

with the initial phase, ϕ_0, and the vector amplitude of $\mathbf{U}_0$. We can ignore the phase offset, and separate the spatial and temporal parts for the forward-propagating field. We want to expand the plane wave function into cylindrical functions, and thus we can apply the technique we used in the last section to solve the boundary condition problem and decompose the bound and radiation modes. The only term that needs to be expanded is the $e^{i\mathbf{k} \cdot \mathbf{r}}$ factor.

We define $\mathbf{k}\cdot\mathbf{r} = (k_\perp \mathbf{e}_{k_\perp} + k_z\mathbf{e}_z)\cdot(r_\perp \mathbf{e}_{r_\perp} + z\mathbf{e}_z) = k_\perp r_\perp \cos(\phi_k - \phi_r) + k_z z = k_\perp r_\perp \cos\Delta\phi + k_z z$, where $\Delta\phi = \phi_k - \phi_r \in [0, 2\pi)$ is the angle between $\mathbf{e}_{k_\perp}$ and $\mathbf{e}_{r_\perp}$. Thus

$$e^{i\mathbf{k}\cdot\mathbf{r}} = e^{ik_\perp r_\perp \cos\Delta\phi} e^{ik_z z} \tag{1.156}$$

is a periodic function of $\Delta\phi$ and hence can be expanded into a Fourier series given below.

$$e^{i\mathbf{k}\cdot\mathbf{r}} = \sum_{m=-\infty}^{\infty} c_m(k_\perp r_\perp) e^{im\Delta\phi} e^{ik_z z}, \tag{1.157}$$

where the coefficients $c_m(k_\perp r_\perp)$ is associated with Bessel's first integral [2]

$$\begin{aligned} c_m(k_\perp r_\perp) &= \frac{1}{2\pi}\int_0^{2\pi} e^{ik_\perp r_\perp \cos\Delta\phi} e^{-im\Delta\phi} \mathrm{d}\Delta\phi & (1.158)\\ &= i^m J_m(k_\perp r_\perp). & (1.159)\end{aligned}$$

Therefore, we have

$$e^{i\mathbf{k}\cdot\mathbf{r}} = \sum_{m=-\infty}^{\infty} i^m e^{im\Delta\phi} e^{ik_z z} J_m(k_\perp r_\perp). \tag{1.160}$$

Notice that the first kind of Bessel's function usually represent standing radial waves, while Hankel functions usually describe travelling waves. Using the relationships that $J_m(k_\perp r_\perp) = H_m^{(1)}(k_\perp r_\perp) + H_m^{(2)}(k_\perp r_\perp)$, we can reexpress the plane wave in terms of incoming (at negative r) and outgoing (at positive r) as below.

$$e^{i\mathbf{k}\cdot\mathbf{r}} = \sum_{m=-\infty}^{\infty} i^m e^{im\Delta\phi} e^{ik_z z} H_m^{(1)}(k_\perp r_\perp) + \sum_{m=-\infty}^{\infty} i^m e^{im\Delta\phi} e^{ik_z z} H_m^{(2)}(k_\perp r_\perp). \tag{1.161}$$

To use the boundary conditions and to separate the bound modes, it is necessary to expand $e^{ik_z z}$ as an integral over β, and to replace $k_\perp$ with $\sqrt{k^2-\beta^2}$. At first glance, it seems both k_z and β have consistent physics meaning and should be exchangable, but can we really do such a replacement?

Work in progress...

[2] see Jackson's E&M, p140, or http://physics.stackexchange.com/questions/44761/plane-wave-expansion-in-cylindrical-coordinates.

Appendix A

Maxwell's Equations of an waveguide

This chapter will dedicate to some fundamental theory of Maxwell's equations. More detailed discussions can be found in Ref.[4]. Some detailed solution of Maxwell's equation applied to cylindrical structures can be found in Ref.[**?**].

For nonmagnetic materials which normally constitute an optical waveguide with $\mu = \mu_0$, the spatial dependence of the electrical field $\boldsymbol{\mathcal{E}}(\mathbf{r})$ and the magnetic field $\boldsymbol{\mathcal{H}}(\mathbf{r})$ of an optical waveguide is determined by Maxwell's equations:

$$\nabla \times \boldsymbol{\mathcal{E}} = i(\mu_0/\varepsilon_0)^{1/2} k \boldsymbol{\mathcal{H}}, \qquad \nabla \times \boldsymbol{\mathcal{H}} = \boldsymbol{\mathcal{J}} - i(\varepsilon_0/\mu_0)^{1/2} k n^2 \boldsymbol{\mathcal{E}}, \tag{A.1}$$

$$\nabla \cdot (n^2 \boldsymbol{\mathcal{E}}) = \rho/\varepsilon_0, \qquad \nabla \cdot \boldsymbol{\mathcal{H}} = 0, \tag{A.2}$$

where $\boldsymbol{\mathcal{J}}$ and ρ are the current density and charge density, $\varepsilon = n^2\varepsilon_0$ is the dielectric constant of the waveguide as a function of space, and $k = 2\pi/\lambda = \omega/c$. We usually assume an implicit time dependence $\exp(-i\omega t)$ in the full field vectors. These equations are written in MKS units, which are used by default.

Sometimes, to avoid the dielectric constant ε_0 and magnetic permeability μ_0 of free space, we can rewrite the Maxwell's equations in Gaussian units, which yield

$$\nabla \times \boldsymbol{\mathcal{E}} = -\frac{1}{c}\frac{\partial \boldsymbol{\mathcal{B}}}{\partial t} = ik\boldsymbol{\mathcal{B}}, \quad \nabla \times \boldsymbol{\mathcal{H}} = \frac{4\pi}{c}\boldsymbol{\mathcal{J}} + \frac{1}{c}\frac{\partial \boldsymbol{\mathcal{D}}}{\partial t} = \frac{4\pi}{c}\boldsymbol{\mathcal{J}} - ik\boldsymbol{\mathcal{D}}, \tag{A.3}$$

$$\nabla \cdot \boldsymbol{\mathcal{D}} = 4\pi\rho, \qquad \nabla \cdot \boldsymbol{\mathcal{B}} = 0, \tag{A.4}$$

where $\boldsymbol{\mathcal{D}} = \varepsilon\boldsymbol{\mathcal{E}}$ and $\boldsymbol{\mathcal{H}} = \boldsymbol{\mathcal{B}}$.

A.1 Fields of translationally invariant waveguides

We define the axis of the waveguide is along z-direction, and the refractive index profile of the waveguide is independent of z, i.e. $n = n(\mathbf{r}_\perp)$, which means the waveguide is translationally invariant. The fields of the waveguide can then be rewritten in a separable form

$$\boldsymbol{\mathcal{E}}(\mathbf{r}) = \boldsymbol{\mathcal{E}}(\mathbf{r}_\perp)\exp(i\beta z), \qquad \boldsymbol{\mathcal{H}}(\mathbf{r}) = \boldsymbol{\mathcal{H}}(\mathbf{r}_\perp)\exp(i\beta z), \tag{A.5}$$

where β is the propagation constant, and $\mathbf{r}_\perp$ is the position vector in the transverse plane perpendicular to the z-axis. We can further decompose these fields into longitudinal and transverse components, parallel and orthogonal to the waveguide axis, respectively, and denoted by subscripts z and $\perp$. That is

$$\boldsymbol{\mathcal{E}}(\mathbf{r}) = (\boldsymbol{\mathcal{E}}_\perp + \mathcal{E}_z\hat{e}_z)\exp(i\beta z), \qquad \boldsymbol{\mathcal{H}}(\mathbf{r}) = (\boldsymbol{\mathcal{H}}_\perp + \mathcal{H}_z\hat{e}_z)\exp(i\beta z) \tag{A.6}$$

Notice that, the sign of β indicates the propagating direction of the fields. By definition, positive and negative β's correspond to forward- and backward-propagating fields.

A.2 Relationships between field components

By substituting Equ. A.6 into the source-free Maxwell equations (Equs. A.1 and A.2 with $\boldsymbol{\mathcal{J}} = 0$, $\rho = 0$), and comparing longitudinal and transverse components, we obtain the relationships between fields components as below

$$\boldsymbol{\mathcal{E}}_\perp = -\left(\frac{\mu_0}{\varepsilon_0}\right)^{1/2}\frac{1}{kn^2}\hat{e}_z \times \left(\beta\boldsymbol{\mathcal{H}}_\perp + i\nabla_\perp\mathcal{H}_z\right), \tag{A.7a}$$

$$\boldsymbol{\mathcal{H}}_\perp = \left(\frac{\varepsilon_0}{\mu_0}\right)^{1/2}\frac{1}{k}\hat{e}_z \times \left(\beta\boldsymbol{\mathcal{E}}_\perp + i\nabla_\perp\mathcal{E}_z\right), \tag{A.7b}$$

$$\mathcal{E}_z = i\left(\frac{\mu_0}{\varepsilon_0}\right)^{1/2}\frac{1}{kn^2}\hat{e}_z \cdot \nabla_\perp \times \boldsymbol{\mathcal{H}}_\perp = \frac{i}{\beta}\left(\nabla_\perp \cdot \boldsymbol{\mathcal{E}}_\perp + (\boldsymbol{\mathcal{E}}_\perp \cdot \nabla_\perp)\ln n^2\right), \tag{A.7c}$$

$$\mathcal{H}_z = -i\left(\frac{\varepsilon_0}{\mu_0}\right)^{1/2}\frac{1}{k}\hat{e}_z \cdot \nabla_\perp \times \boldsymbol{\mathcal{E}}_\perp = \frac{i}{\beta}\nabla_\perp \cdot \boldsymbol{\mathcal{H}}_\perp. \tag{A.7d}$$

Now we consider the waveguide of cylindrical fiber case. Due to symmetry, we tend to use the cylindrical coordinate system, which gives

$$\nabla_\perp = \hat{r}_\perp\frac{\partial}{\partial r_\perp} + \hat{\phi}\frac{1}{r_\perp}\frac{\partial}{\partial\phi}. \tag{A.8}$$

Therefore, Equ. A.7 implies that the transverse components can be expressed in terms of the longitudinal components by

$$\mathcal{E}_{r_\perp} = \frac{i}{h^2}\left[\beta\frac{\partial\mathcal{E}_z}{\partial r_\perp} + \left(\frac{\mu_0}{\varepsilon_0}\right)^{1/2}\frac{k}{r_\perp}\frac{\partial\mathcal{H}_z}{\partial\phi}\right], \tag{A.9a}$$

$$\mathcal{E}_\phi = \frac{i}{h^2}\left[\frac{\beta}{r_\perp}\frac{\partial\mathcal{E}_z}{\partial\phi} - \left(\frac{\mu_0}{\varepsilon_0}\right)^{1/2}k\frac{\partial\mathcal{H}_z}{\partial r_\perp}\right], \tag{A.9b}$$

$$\mathcal{H}_{r_\perp} = \frac{i}{h^2}\left[\beta\frac{\partial \mathcal{H}_z}{\partial r_\perp} - \left(\frac{\varepsilon_0}{\mu_0}\right)^{1/2}\frac{kn^2}{r_\perp}\frac{\partial \mathcal{E}_z}{\partial \phi}\right], \tag{A.9c}$$

$$\mathcal{H}_{\phi} = \frac{i}{h^2}\left[\frac{\beta}{r_\perp}\frac{\partial \mathcal{H}_z}{\partial \phi} + \left(\frac{\varepsilon_0}{\mu_0}\right)^{1/2} kn^2\frac{\partial \mathcal{E}_z}{\partial r_\perp}\right], \tag{A.9d}$$

with $h^2 = k^2n^2 - \beta^2 = k^2\varepsilon_f - \beta^2$ and $n = n(\mathbf{r}_\perp)$.

Correspondingly, the component relationships in Gauss units are

$$\mathcal{E}_{r_\perp} = \frac{i}{h^2}\left[\beta\frac{\partial \mathcal{E}_z}{\partial r_\perp} + \frac{k}{r_\perp}\frac{\partial \mathcal{H}_z}{\partial \phi}\right] = \frac{i\beta}{h^2}\frac{\partial \mathcal{E}_z}{\partial r_\perp} - \frac{km}{r_\perp h^2}\mathcal{H}_z, \tag{A.10a}$$

$$\mathcal{E}_{\phi} = \frac{i}{h^2}\left[\frac{\beta}{r_\perp}\frac{\partial \mathcal{E}_z}{\partial \phi} - k\frac{\partial \mathcal{H}_z}{\partial r_\perp}\right] = -\frac{\beta m}{r_\perp h^2}\mathcal{E}_z - \frac{ik}{h^2}\frac{\partial \mathcal{H}_z}{\partial r_\perp}, \tag{A.10b}$$

$$\mathcal{H}_{r_\perp} = \frac{i}{h^2}\left[\beta\frac{\partial \mathcal{H}_z}{\partial r_\perp} - \frac{kn^2}{r_\perp}\frac{\partial \mathcal{E}_z}{\partial \phi}\right] = \frac{i\beta}{h^2}\frac{\partial \mathcal{H}_z}{\partial r_\perp} + \frac{kn^2 m}{r_\perp h^2}\mathcal{E}_z, \tag{A.10c}$$

$$\mathcal{H}_{\phi} = \frac{i}{h^2}\left[\frac{\beta}{r_\perp}\frac{\partial \mathcal{H}_z}{\partial \phi} + kn^2\frac{\partial \mathcal{E}_z}{\partial r_\perp}\right] = -\frac{\beta m}{r_\perp h^2}\mathcal{H}_z + \frac{ikn^2}{h^2}\frac{\partial \mathcal{E}_z}{\partial r_\perp}. \tag{A.10d}$$

Vector and Scalar operators...

Vector wave equations...

In Gauss units, we have

$$-\nabla\times(\nabla\times\mathbf{E}) - \frac{\varepsilon}{c^2}\frac{\partial^2\mathbf{E}}{\partial t^2} = -\frac{4\pi}{c}\mathbf{J}. \tag{A.11}$$

We can further simplify the equation above by using

$$\nabla\times(\nabla\times\boldsymbol{\mathcal{E}}) = -\nabla(\nabla\cdot\boldsymbol{\mathcal{E}}) + \nabla^2\boldsymbol{\mathcal{E}} \tag{A.12}$$

$$-\frac{\varepsilon}{c^2}\frac{\partial^2\mathbf{E}}{\partial t^2} = \frac{\varepsilon\omega^2}{c^2}\frac{\partial^2\boldsymbol{\mathcal{E}}}{\partial t^2}. \tag{A.13}$$

Bibliography

[1] Clement Lacroûte, KS Choi, A Goban, DJ Alton, D Ding, NP Stern, and HJ Kimble. A state-insensitive, compensated nanofiber trap. *New Journal of Physics*, 14(2):023056, 2012.

[2] Fam Le Kien, V. I. Balykin, and K. Hakuta. Atom trap and waveguide using a two-color evanescent light field around a subwavelength-diameter optical fiber. *Phys. Rev. A*, 70:063403, Dec 2004.

[3] Eugen Vetsch. *Optical interface based on a nanofiber atom-trap*. PhD thesis, Johannes Gutenberg-Universitat in Mainz, 2010.

[4] Allan W Snyder and J Love. *Optical waveguide theory*, volume 190. Springer, 1983.

[5] Vasily V Klimov and Martial Ducloy. Spontaneous emission rate of an excited atom placed near a nanofiber. *Physical Review A*, 69(1):013812, 2004.

[6] H Nha and W Jhe. Cavity quantum electrodynamics for a cylinder: inside a hollow dielectric and near a solid dielectric cylinder. *Physical Review A*, 56(3):2213, 1997.

Index